

Subduction and slab detachment under moving trenches during ongoing India-Asia convergence

Abdul Qayyum^{a*}, Nalan Lom^a, Eldert L. Advokaat^b, Wim Spakman^a,
Douwe G. van der Meer^a, Douwe J.J.van Hinsbergen^a

^a Department of Earth Sciences, Utrecht University, Princetonlaan 8a, 3584 CB, Utrecht, the Netherlands

^b School of Geography, Earth and Environmental Sciences, University of Birmingham, B15 2TT, UK

*Corresponding author: Abdul Qayyum (geologist.aqayyum@gmail.com)

16 Abstract

17 The dynamics of slab detachment and associated geological fingerprints have been inferred from
 18 various numerical and analogue models. These invariably use a setup with slab-pull-driven convergence
 19 in which a slab detaches below a mantle-stationary trench after the arrest of plate convergence due to
 20 arrival of continental lithosphere. In contrast, geological reconstructions show that post-detachment
 21 plate convergence is common and that trenches and sutures are rarely mantle-stationary during
 22 detachment. Here, we identify the more realistic kinematic context of slab detachment using the
 23 example of the India-Asia convergent system. We first show that only the India and Himalayas slabs
 24 (from India's northern margin) and the Carlsberg slab (from the western margin) unequivocally
 25 detached from Indian lithosphere. Several other slabs below the Indian Ocean do not require a
 26 Neotethyan origin and may be of Mesotethys and Paleotethys origin. Additionally, the still-connected
 27 slabs are being dragged together with the Indian plate forward (Hindu Kush) or sideways (Burma,
 28 Chaman) through the mantle. We show that Indian slab detachment occurred at moving trenches during
 29 ongoing plate convergence, providing more realistic geodynamic conditions for use in future numerical
 30 and analogue experiments. We identify that the actively detaching Hindu Kush slab is a type-example
 31 of this setting, whilst a 25-13 Ma phase of shallow detachment of the Himalayas slab, here reconstructed
 32 from plate kinematics and tomography, agrees well with independent, published geological estimates
 33 from the Himalayas orogen of slab detachment. The Sulaiman Ranges of Pakistan may hold the
 34 geological signatures of detachment of the laterally dragged Carlsberg slab.

35

36 1. INTRODUCTION

37 If negative buoyancy of subducted lithosphere pulling slabs into the mantle is the prime driver of
 38 plate tectonics, as widely thought (Conrad & Lithgow-Bertelloni, 2002; Forsyth & Uyedat, 1975;
 39 Lithgow-bertelloni & Richards, 1998a), the detachment of a slab from a surface plate is a key event to
 40 calibrate the drivers of plate motion (Fernández-García et al., 2019; van Hunen and Allen, 2011;
 41 Bercovici et al., 2015; Duretz et al., 2011). Because slab detachment occurs at depth and is not an
 42 instantaneous process it cannot be directly constrained from geophysical or geological observations
 43 (Duretz et al., 2014; van Hunen & Allen, 2011; Wortel & Spakman, 2000). For that reason snap shot
 44 observations from e.g., seismic tomography, or earthquake focal mechanisms, in regions where the
 45 process may be presently active (e.g., the Hindu Kush (Kufner et al., 2017), the southern Banda Arc
 46 (Ely & Sandiford, 2010), the south-eastern Carpathians (Sperner et al., 2001), or the central-eastern
 47 Betics (Spakman et al. 2018) are complemented with inferences made from numerical and analogue

experiments. For those experiments, however, it is important to first identify if they can represent the natural example under investigation.

Earliest analogue and numerical experiments (Buiter et al., 2002; Buiter & Pfiffner, 2003; Chemenda et al., 1995; Taras V. Gerya et al., 2004; Yoshioka & Wortel, 1995; van de Zedde & Wortel, 2001) were designed to evaluate whether slab detachment would be a physically plausible explanation for geological observations such as transient surface uplift, heating, and magmatism, in regions where seismological inference suggests that a slab has broken off (Davies & von Blanckenburg, 1995; Maury et al., 2002; van der Meulen et al., 1998; Wortel & Spakman, 1992, 2000). Subsequent models have become more advanced and were expanded to 3D (Duretz et al., 2014; Duretz et al., 2011; van Hunen & Allen, 2011; Regard et al., 2008; Yoshioka & Wortel, 1995). Dynamic transient topographic changes, high-temperature metamorphism, and magmatism have since become widely used as signature events to date suspected slab break-off phases (Atherton & Ghani, 2002; Kohn et al., 2002; Zhen Li et al., 2014; Maheo et al., 2002; Vissers et al., 2016; Yuan et al., 2010). However, as Garzanti et al. (2018) recently wrote: “slab breakoff has been invoked in so many settings and time frames that it could have hardly taken place in each and every case in which it was called upon”. In other words, the geological observations that are widely considered as signatures of slab detachment are likely equivocal and cannot be called unique identifiers of the process.

Importantly, models of slab detachment published so far invariably assume a very specific geodynamic setting involving a mantle stationary trench at which plate convergence as well as absolute plate motion come to halt when continental lithosphere enters the trench (e.g., Duretz et al., 2011; van Hunen & Allen, 2011; van de Zedde & Wortel, 2001). After this, the hanging and steepening slab gradually detaches by shearing and necking (e.g., Duretz et al. 2012) due to the still active slab pull. Following detachment the detached slabs sink vertically below the mantle-stationary suture (Figure 1) (Běhounková & Čížková, 2008; Billen, 2010; Duretz et al., 2011; Gerya et al., 2004; González & Negredo, 2012; van Hunen & Allen, 2011; Lee & King, 2011). In contrast, in almost all natural cases where slab detachment occurred in the last tens of millions of years, plate convergence continued long after detachment. In addition, the trenches at which detachment occurred, as well as the upper and lower plates, kept moving relative to the mantle (Agard et al., 2011a; Hafkenscheid et al., 2006; van Hinsbergen et al., 2019, 2020a; van de Lagemaat et al., 2018; Parsons et al., 2020; Schellart & Spakman, 2015), consequently leading to suture zones across the globe that are typically offset relative to their corresponding, detached slabs (Domeier et al., 2016; van der Meer et al., 2010; 2018; Schellart & Spakman, 2015; Vissers et al., 2016). Therefore, if the process of slab detachment occurs while relative and absolute plate motion is ongoing, this may influence the dynamics of the process and perhaps may entail different geological responses than inferred from the detachment modelling so far.

A prime example where slab detachment occurred during ongoing plate convergence is at subduction zone(s) that consumed Indian plate lithosphere during convergence with Asia. Seismological studies have revealed that (except for the far north-western corner in the Hindu Kush, Kufner et al., 2017) there is currently no subducting slab attached to northern India (Agius & Lebedev, 2013; Chen et al., 2017; Nábelek et al., 2009; Replumaz et al., 2010; Van Der Voo et al., 1999), yet thousands of km of India-Asia convergence occurred since Cretaceous time and must have been accommodated by subduction (Molnar & tapponnier, 1975; Patriat & Achache, 1984). Even today, the absolute northward Indian plate motion and relative India-Asia convergence continues, with a steady northward pace that has been ~4 cm/a for the last 13 Ma (Copley et al., 2010; DeMets & Merkouriev, 2021; van Hinsbergen et al., 2011; Molnar & Stock, 2009).

The mantle below India and Indian Ocean was among the first regions where deep mantle structure was correlated to subduction history (Hafkenscheid et al., 2006; Replumaz et al., 2004; Van Der Voo et al., 1999). These studies identified multiple detached slabs, and the shallowest of these are identified hundreds to more than 1500 km to the south of the modern northern extent of the Indian continental lithosphere which is imaged sub-horizontally below Tibet over a distance of 300-800 km north of the modern plate boundary, the southern Himalayan front (Agius & Lebedev, 2013; Chen et al., 2017; van Hinsbergen et al., 2019) (Figure 2). Clearly, these geodynamic constraints differ completely from those used for the past numerical models simulating slab detachment and from which the currently perceived diagnostic geological signatures of slab detachment are derived.

In this paper, we aim to investigate the kinematic history of slab detachment events during ongoing Indian plate subduction and convergence. To this end, we first need to evaluate which of the previously identified anomalies are likely representing subducted (Neotethyan) lithosphere that detached from the Indian plate, rather than from older plates whose relics are now found in Tibet. Ever since the first interpretation of van der Voo et al. (1999) all lithosphere below India has been interpreted as Neotethyan oceanic lithosphere that detached from the Indian continental margin since the Cretaceous. However, global correlations between slabs and geological records have since then shown that anomalies in the deep mantle may represent slabs that subducted in the Permo-Triassic and Jurassic (van der Meer et al., 2010; 2018; Sigloch & Mihalynuk, 2013). Part of the slabs below the Indian Plate that were previously interpreted as Neotethyan may thus well relate to earlier, Permo-Triassic to Early Cretaceous subduction of which the corresponding geological records are located in the Mesozoic geology of accreted blocks that are now found in the Tibetan Plateau. From the anomalies that are most likely Neotethyan, we then evaluate previous estimates of the timing of detachment from the Indian plate and evaluate to what extent the conditions under which detachment occurred, differ from classical concepts. Finally, we evaluate the effects that ongoing motion during slab detachment may conceptually have on the mechanism of detachment, evaluate whether the detachment events may have first-order expressions in the geological record, and determine a set of geodynamic conditions and case study areas

for future modelling experiments to evaluate what geological observations may be diagnostic for slab detachment while the slab is being dragged by, and in the direction of the absolute motion of the lower plate.

2. Identifying Neotethyan subducted slabs below India

2.1 Context: global correlations between seismic tomography and geology

With the development of global seismic mantle tomography towards more detailed imaging of slabs and their remnants, now some 25 years ago (Bijwaard et al., 1998; van der Hilst et al., 1997; Grand et al., 1997), came the opportunity to infer the current deep mantle locations of lithosphere that once subducted at still-active, or former and now inactive paleo-subduction zones. In the ten years prior, upper mantle slabs had been correlated to mostly active subduction zones e.g., (Fukao et al., 1992; Hilst et al., 1991; Spakman et al., 1988), and the first lower-mantle anomalies became correlated to subducted oceanic lithosphere predicted by plate reconstructions in the Tethyan and Pacific realms (Duretz et al., 2014; Fukao et al., 2001; Grand et al., 1997; Hafkenscheid et al., 2006; van Hinsbergen et al., 2005; Lippert et al., 2014; Lithgow-Bertelloni & Richards, 1998b; Replumaz & Tapponnier, 2003; Richards & Engebretson, 1990; Van Der Voo et al., 1999). A next development was the reconstruction of the ‘mantle memory’ of subduction through systematic correlation between remnants of detached slabs in the mantle and locations of paleo-subduction in plate tectonic reconstruction models (van der Meer et al., 2010). This revealed that increasingly deeper slabs tend to be well-explained by increasingly older subduction zones, with Cenozoic subduction mostly restricted to the upper mantle, and top of the lower mantle, and slabs on the core-mantle boundary correlating to Permo-Triassic slabs (Butterworth et al., 2014; Domeier et al., 2016; van der Meer et al., 2010; 2018; Sigloch & Mihalynuk, 2013). The correlations moreover showed that in general, detached sinking slabs do not tend to move laterally relative to each other (van der Meer et al., 2018), and sink more or less vertically through the mantle (Domeier et al., 2016).

In contrast, slabs can and do move laterally through the mantle when they are still attached to surface plates, as suggested by the reconstructions of moving trenches in absolute plate motion models (Hall & Spakman, 2002; van de Lagemaat et al., 2018; Lallemand et al., 2008; Parsons et al., 2021; Schellart, 2008; Schellart & Spakman, 2015; Sdrolias & Müller, 2006). Sigloch and Mihalynuk (2013) argued that the shape of slabs imaged in seismic tomography contains valuable information on the absolute motion that their corresponding trenches underwent during subduction. Schepers et al. (2017) and Boschman et al. (2018) slightly modified this concept to include effects of periods of flat slab subduction and argued that slab shape reflects the absolute motion of the location where the slab bended into the mantle during its subduction, whereby the slab bend and trench may be offset by a flat slab

segment that may vary in width through time. These concepts predict that during subduction with mantle-stationary slab bends, slabs tend to form near-vertical walls of thickened/folded slab in the mantle transition zone while sinking into the lower mantle (Figure 4a-c). At retreating slab bends (i.e. roll-back), however, slabs tend to drape on the 660 km discontinuity and become flat-lying (e.g., van der Hilst et al. 1993) (Figure 4 d-f). Advancing slab bends lead to overturned slabs (Figure 4g-i)(van Hinsbergen et al., 2019; Van Der Voo et al., 1999). These flat-lying slabs will eventually also sink vertically through the mantle while maintaining their shape (Boschman et al., 2018), causing that their average sinking rate from the moment of detachment tends to be reduced as compared to slabs sinking below a mantle-stationary trench (van der Meer et al. 2018). A current example is the Izu-Bonin slab that is subducting at a retreating part of the Izu-Bonin-Marianas trench and that is mostly overlying the 660 km discontinuity (e.g. van der Hilst et al. 1993; van der Hilst and Seno 1993), whereas in the south where the trench has been more mantle-stationary, the Marianas slab reached as deep as 1200 km (van der Hilst and Seno 1993; Miller et al., 2005; Wu et al., 2016). Moreover, while actively subducting slabs may be dragged sideways by the absolute motion of the downgoing plate at the trench, over distances in excess of 1000 km (van de Lagemaat et al., 2018; Parsons et al., 2021; Spakman et al., 2018) implying that the modern location of slab remnants in the mantle is a reasonable marker for where slabs detached, but not necessarily where they started their subduction.

2.2 Geological constraints on ocean closure in Tibet

We aim to identify the location and shape of slabs that detached from the Indian plate during its northward motion towards Eurasia since the Early Cretaceous. The relationships summarized above then require that we distinguish these Cretaceous and younger slabs from other slabs that were subducted in Permo-Triassic to Early Cretaceous time that globally tend to be in the lower to mid-mantle(van der Meer et al., 2018; van Der Meer et al., 2010), depending on their history of subduction.

The geological record of Tibet and the Himalayas shows evidence for multiple subduction zones that have been active at times between the Permian times to the present zones (Figure 2,3,8). The youngest record of subduction and accretion in the system is the Cenozoic Himalayan accretionary orogen, which forms an incomplete, thrust, and often metamorphosed record of continent-derived, mostly sedimentary units stripped off their subducted or otherwise deep under thrust lower crustal and mantle lithospheric underpinnings (van Hinsbergen & Schouten, 2021; Hodges, 2000; Kapp & DeCelles, 2019). The Himalayas is bounded to the north by the Indus-Yarlung (Tsangpo) suture zone with relics of Triassic ‘*Neotethys*’ ocean floor that subducted northward since at least Early Cretaceous time (~130 Ma) below the Lhasa terrane of southern Tibet (Hébert et al., 2012; Kapp and Decelles, 2019; Maffione et al., 2015). In this time interval (since at least Early Cretaceous time) the net amount of convergence between India and Asia was ~8000 km (Figure 3). Tibetan shortening started already

in Cretaceous time and amounted a few hundred kilometres (van Hinsbergen et al., 2011; Kapp et al., 2005; Murphy et al., 1997) and between ~50 Ma and the present, Tibetan shortening, in the east aided by extrusion of Indo-China, led to ~1000-1200 km of northward indentation of the India-Eurasia plate boundary (Replumaz & Tapponnier 2003, Royden *et al.* 2008, van Hinsbergen *et al.* 2011, 2019; Ingalls *et al.* 2016), and a minimum of ~6500-7000 km of lithosphere must this have been consumed by subduction. Seismic tomography studies have shown that at present, Indian continental lithosphere lies horizontally directly below southern Tibetan crust, and thus interpreted that mantle lithosphere that originally underpinned Tibetan crust must have been lost to delamination (Nábelek et al., 2009). This delaminated lithosphere may thus also contribute to, presumably small-scale, seismic velocity anomalies below Tibet (Replumaz et al., 2013).

The Lhasa terrane is separated by the Bangong-Nujiang suture from the Qiangtang terrane (Figure 2). The geological record of the suture zone, as well as paleomagnetic constraints from the Lhasa and Qiangtang terranes, reveal that this suture accommodated the closure of a once ~6000 km wide '*Mesotethys*' ocean between the late Triassic and early Cretaceous (Figure 3,8) (Kapp & Decelles, 2019; S. Li et al., 2019; Zhenyu Li et al., 2016; Yin & Harrison, 2000). Contemporaneous arc magmatic rocks on both sides of the suture zone, and the structure of the suture zone itself, have been interpreted to show that closure of the Mesotethys ocean was likely accommodated by double sided subduction (Luo & Fan, 2020; Zhu et al., 2016). Alternatively, Kapp and DeCelles (2019) inferred that all magmatism on Lhasa since the Triassic resulted from northward Neotethys subduction along its southern margin and that Mesotethys closure was entirely accommodated by northward subduction below Qiangtang.

The Qiangtang terrane is separated from NE Tibetan terranes by the Songpan-Garzi accretionary prism (Figure 2) that consists mostly of accreted Permo-Triassic clastic sedimentary rocks thought to have derived from subducted '*Paleotethys*' ocean floor. Paleomagnetic data show that the Paleotethys was of similar width as the Meso- and Neotethys, on the order of 6000 km, and closed throughout the Permo-Triassic time (Figure 3) (Song et al., 2017). Contemporaneous arcs on either side of the subduction zone, and tectonic architecture show that also this closure was likely associated with double-sided subduction (Kapp & Decelles, 2019). Sutures within NE Tibet predate the Mesozoic and predate the reconstructed mantle memory (van der Meer et al., 2018). These terranes have moved together with the North China block since Paleozoic time, until late Cenozoic shortening during Tibetan plateau growth (Wu et al., 2016; Yin & Harrison, 2000).

Based on global correlations between slabs and geologically reconstructed subduction zones (Butterworth et al., 2014; van der Meer et al., 2010; 2018; Sigloch & Mihalynuk, 2013), we expect that slabs related to Paleotethys, Mesotethys, and Neotethys subduction are still visible in the mantle. And because the three oceans had similar width (Figure 3), the associated seismic velocity anomalies are

expected to have roughly similar volumes, if there was no additional crustal production from mid-ocean-ridge spreading. We use this as a guide in our interpretation: variations in volume may also be due to differences in tomographic resolution, resolved seismic velocity amplitudes (Hafkenscheid et al. 2006) and volume changes as result of compression and phase changes during sinking into the deep mantle (Van Der Meer et al., 2014).

The closure of one ocean basin may be accommodated by multiple slabs, as has been argued for Mesotethys and Paleotethys closure (see above). Reconstructions of Neotethys subduction history include models that interpret (i) a single subduction zone that remained more or less mantle-stationary along southern Tibet since the Early Cretaceous (van Hinsbergen et al., 2019), (ii) a single subduction zone that rolled back from the Tibetan margin to an equatorial position in the Cretaceous that came to an arrest during Late Cretaceous (Hafkenscheid et al., 2006) or Paleocene (Kapp & Decelles, 2019) arrival of the Indian margin in the trench, followed by renewed subduction along the Eurasian margin; (iii) a double subduction zone including one along southern Tibet and an intra-oceanic one that started in the Early Cretaceous at the equator and that remained active until Cretaceous or Eocene arrival of India in the trench (Tapponnier et al., 1981; Aitchison et al., 2007, van Hinsbergen et al., 2012), or advanced towards the south Tibetan margin in the Eocene (Jagoutz et al., 2015; Martin et al., 2020). The latter scenario suggests that even though subduction started at the equator, the slab was dragged northward through the mantle during subduction and detached close to the southern Eurasian margin. Interpretations of when continental lithosphere arrives at the south Tibetan trench vary considerably (see overview in e.g., (Parsons et al., 2020), but only impact the type of lithosphere that is consumed by subduction and underthrusting, but not the amount, and the differences in collision age between these models are hence not of importance to our kinematic analysis and tomographic interpretation.

Finally, the geological record and plate reconstructions reveal evidence for west- and east-ward subduction of Indian plate lithosphere during India's northward flight. Westward subduction is reconstructed and documented from the Sulaiman ranges orogen and overlying ophiolites in Pakistan and occurred from ~70 Ma until the Eocene, followed by oblique underthrusting of west India below Eurasia occurred in the Neogene (Gaina et al., 2015; Gnos et al., 1998). The latter deformation is partitioned over the Sulaiman ranges fold-thrust belt and the left-lateral Chaman Fault that together form the western plate boundary of Indian plate (Figure 2). To the east, subduction occurred below the Andaman Islands and the West Burma Block since the Cretaceous (Plunder et al., 2020; Westerweel et al., 2019; Bandopadhyay et al., 2021), and became increasingly more oblique upon northward migration of the India-Asia plate boundary due to shortening in Tibet (van Hinsbergen et al., 2011; 2019). Also here, deformation is partitioned over a frontal fold-thrust belt (the Indo-Burman ranges and the Andaman-Nicobar accretionary wedge) and a transform system (the right-lateral Sagaing-Andaman Sea-Sumatran Fault system) (e.g., Morley & Arboit, 2019) (Figure 2).

2.3. Absolute plate motions: where to search and what to search for?

Searching for the anomalies that correspond to the closure of the Tethyan oceans requires constraints on absolute plate motion (i.e., relative to the mantle) of India and Asia. True polar wander-corrected paleomagnetic reference frames suggest that Eurasia did not move appreciably in absolute latitude since the Jurassic (Torsvik et al., 2012), and when adding paleomagnetism-based pre-Cretaceous reconstructions of North China (and Tibetan units accreted to that) relative to Siberia, the absolute paleolatitude of Tibet is about latitudinally stable before that time as well (Torsvik et al., 2012; Van Der Voo et al., 2015; Torsvik and Cocks, 2017)(Figure 3). Absolute plate motions back to Cretaceous time are reasonably well constrained by hotspot reference frames (Dobrovine et al., 2012; Torsvik et al., 2019). Prior to the Cretaceous, paleolongitudinal control is more challenging, but global correlations between subduction zones and slabs (Van der Meer et al., 2018; Van Der Meer et al., 2010), or between intraplate volcanics correlated to stationary plume-generation-zones at the core-mantle boundary (Burke et al., 2008; Torsvik et al., 2014) suggest that Eurasia also did not move much in paleolongitude since the Triassic. Consequently, assuming vertical sinking of slab remnants, the lithosphere that was consumed by Paleo-, Meso-, and Neotethys subduction is generally expected to be still located below the Indian plate and Tibet today (Hafkenscheid et al., 2006; van der Meer et al., 2018; Parsons et al., 2020; Van Der Voo et al., 1999).

With Eurasia as more or less mantle-stationary, the Tethyan oceans closing during absolute northward motion of plates carrying the (micro-)continents of Qiangtang, Lhasa, and India, and using the subduction polarities interpreted from geology as summarized above, we may predict mantle structure that results from the various scenarios using the relationship between absolute trench motion and resulting slab geometry. Southward subduction below the Qiangtang and Lhasa terranes during their northward flights in the Permo-Triassic, and Triassic-Early Cretaceous, respectively, should have been associated with slab roll-back and predict flat-lying slabs of a few thousand km wide below much of the Indian Plate. If subduction was northward below the Lhasa terrane during its northward motion (Kapp & Decelles, 2019), the trench would have advanced and a flat-lying slab is also expected, although this slab would be overturned. Northward subduction of the Paleotethys below NE Tibet and of the Mesotethys below Qiangtang would have formed slab walls. Near-stationary Neotethys subduction below southern Tibet in Cretaceous to Eocene time would generate a slab wall, whereas the ~1000 km of northward trench advance associated with Tibetan shortening since the Eocene would result in overturned and flat(ter) lying slabs if lithosphere subducted, and/or horizontally underthrust lithosphere below Eurasia, if deep subduction was prohibited by excess buoyancy of the underthrusting lithosphere. Equatorial subduction preceded by slab retreat (Hafkenscheid et al., 2006; Kapp &

Decelles, 2019) or followed by slab advance (Jagoutz et al., 2015; Martin et al., 2020) would lead to flat-lying slabs south of the main slab wall of south Tibetan subduction, whereas mantle-stationary equatorial subduction in the Neotethys (Tapponnier et al., 1980; Aitchison et al., 2007; van Hinsbergen et al., 2012) would produce a second slab wall along-side the one forming along southern Tibet (Figure 8). Finally, slabs that subducted west and east of India in Cretaceous to Cenozoic time must have undergone northward, more or less slab-strike parallel dragging as long as they were attached to the moving Indian lithosphere, or should have been left behind and sinking vertically at the location of their detachment (Le Dain et al., 1984; van de Lagemaat et al., 2018; Parsons et al., 2021; Spakman et al., 2018).

3. Seismic tomographic constraints on mantle structure

3.1 Approach

The first study of seismic tomographic images of the mantle below India and Tibet was conducted by van der Voo et al. (1999). Together with subsequent studies about a dozen anomalies have now been identified (Hafkenscheid et al., 2006; van der Meer et al., 2010; 2018; Negredo et al., 2007; Parsons et al., 2020; Replumaz et al., 2010; 2014). The number of tomographic anomalies in the mantle below India and Tibet is far greater than the number of ocean basins that was consumed, from which it follows that there are more slab detachment phases than continental collisions.

The initial studies of van der Voo et al. (1999), Replumaz et al. (2004), and Hafkenscheid et al. (2006) assumed that all slabs below southern Tibet and India represented Neotethyan lithosphere that subducted in Cretaceous and younger time. Only subducted slabs in the lower mantle below Tibet, to the north of the Indus-Yarlung suture between India and Asia, were interpreted by these authors as relicts of the Mesotethys or Paleotethys oceans that subducted before Early Cretaceous time (Figure 2,8). Even though in the decade that followed global tomography-geology connections have shown that also Triassic and Jurassic subducted slabs are typically still visible in the lower mantle (van der Meer et al., 2010; 2018; Sigloch & Mihalynuk, 2013) all studies of anomalies in the mantle below India still assume all of these are Neotethyan (Parsons et al., 2020).

As basis for our re-evaluation of Tethyan slabs, we use the nomenclature of slabs as defined in the Atlas of the Underworld compilation of tomographic anomalies of van der Meer et al. (2018), which includes all anomalies that had previously been interpreted as subducted slabs. This nomenclature names anomalies after presently overlying geographic features instead of after the lithosphere/basin that they are interpreted to represent. This objectively labels the anomalies and leaves freedom for interpretation. We refer the reader to this document for names that have been used by previous workers and note that Parsons et al. (2020) recently labelled these anomalies differently.

In addition to the compilation of van der Meer et al. (2018), we include one previously identified anomaly below Tibet described by Replumaz et al. (2013) (their AF anomaly that they interpreted as delaminated Tibetan lithosphere rather than a subducted slab) and identify several anomalies that have not previously been described, in the shallow upper mantle and in the deepest lower mantle. We use the UU-P07 P-wave tomographic model (Amaru, 2007; Hall & Spakman, 2015) that was also used by van der Meer et al. (2018), and in addition analyse velocity maps (Shephard et al., 2017) to evaluate the occurrence of the identified anomalies across tomographic models (Figure 2, Figure 3). In the following paragraphs, we navigate through mantle structure below India and Tibet from the largest anomaly that has so far been interpreted as the main body of Neotethyan lithosphere, and from there correlate shallower and deeper slabs as Neotethyan, Mesotethyan, and Paleotethyan slabs.

3.2 Slabs below India and Tibet and their previous interpretations

The most prominent tomographic anomaly in the mantle below India is the *India slab* (Figure 5,6). In the west, the India slab is found around 700-1600 km depth, becomes deeper (1000-1800 km) below central India, and shallower again towards the east (700-1600 km). It has a N-S width of up to 1500 km suggesting major thickening. The anomaly is striking NW-SE (Figure 5,6), at the location where in the mantle frame of reference (Dobrovine 2012) the southern Tibetan active margin is restored in Cretaceous to Eocene time (van Hinsbergen et al., 2019; Replumaz et al., 2004; Royden et al., 2008). Ever since its first identification by van der Voo et al. (1999), the India anomaly has consistently been interpreted as the main body of Neotethyan lithosphere that subducted at a trench along the Cretaceous to Paleogene south Tibetan margin. The India slab is overall more or less vertically aligned as a slab wall (Sigloch & Mihalynuk, 2013). Tectonic reconstructions supported by paleomagnetic data and placed in a mantle frame of reference (Dobrovine et al., 2012) suggest that this trench advanced over some 500 km during the late Cretaceous to early Eocene (van Hinsbergen et al., 2019; Lippert et al., 2014). This advance is likely too small to be tomographically detected in the blurred image of the thickened/buckled slab remnant. The vertical extent of the slab is an order of magnitude smaller than the amount of early Cretaceous to Eocene India-Asia convergence, and if this slab hosts the main body of Neotethyan lithosphere, it must have thickened, e.g., by buckling and/or lateral spreading. At peak convergence rates in excess of 20 cm/a (DeMets & Merkouriev, 2021), may have contributed to thickening upon entering the lower mantle.

To the north of the India slab, at a shallower depth of 400-800 km, the *Himalayas slab* is found (HM: Figure 5,7). Along-strike, the slab varies in orientation from vertical to south-dipping, the latter interpreted as an overturned orientation (Replumaz et al., 2010). The Himalayas slab is at its largest, and its base is at its deepest, below the central part of the Indian continent and becomes shallower towards the east and west. The shallowest part of top of the Himalayas slab is located below the central-

eastern Himalayas (Figure 5,6). The Himalayas slab is detached and offset northward from the Indian slab even though it is interpreted to have subducted below southern Tibet along Himalayan thrusts (Van Hinsbergen et al., 2012; Parsons et al., 2021; Replumaz et al., 2010). Its overturned position and northward offset relative to the Indian plate are interpreted to reflect subduction during northward trench advance accommodated by Cenozoic shortening and extrusion in the Tibetan plateau (van Hinsbergen et al., 2019; Replumaz et al., 2010). This slab is interpreted to be the youngest slab to have detached from the northern Indian margin (Replumaz et al., 2010; 2004).

The northern margin of *Indian plate lithosphere* that is horizontally underthrust directly below the Tibetan Plateau crust (Chen et al., 2017; Nábelek et al., 2009) protrudes northward from the Himalayan thrust front, over a distance that varies along strike from ~800 km near the syntaxes, to ~400 km from the east-central Himalayas to the north (Agius & Lebedev, 2013; van Hinsbergen et al., 2019). The northern edge of this horizontally underthrust lithosphere is offset northward from the detached Himalayas slab (Figure 6), which must reflect the amount of absolute northward motion of the Indian plate after detachment (van Hinsbergen et al., 2019).

Below the Hindu Kush, to the west of the western Himalayan syntaxis, the *Hindu Kush* slab is located (HK; Figure 5). The slab is interpreted as oceanic lithosphere that is still attached to the north-western Indian continental margin, but that lies buried below the Sulaiman Ranges of Pakistan (Kufner et al., 2017). It is a N-dipping, E-W trending, near-vertical anomaly that reaches a depth of ~600 km below Hindu Kush region in North Pakistan (Kufner et al., 2017; C. Li & Hilst, 2010; Negrodo et al., 2007; Replumaz et al., 2010; Van Der Voo et al., 1999) and is offset northward relative to the Himalayas slab by a few hundred km (Figure 2). Detailed seismological studies have shown that the slab is currently in the process of detaching (Kufner et al., 2017, 2021; Lister et al., 2008).

In the east, the *Burma slab* is imaged as a N-S striking, steeply-east-dipping anomaly under the west Burma Block of Myanmar, still connected to the northward moving Indian plate (Figure 5,7). This upper mantle slab has been recognized in many earlier studies and is disconnected by a slab window below the Andaman Sea from the Sunda slab below Sumatra and Java (Huang and Zhao, 2006; Li et al., 2008; Replumaz et al., 2010; Zhao and Ohtani, 2009; Parsons et al., 2021). The Burma slab has accommodated the E-W convergence component of the highly oblique subduction between India and Sundaland (Figure 2), which amounted ~600 km since ~40 Ma (van Hinsbergen et al., 2011). A mirror image of the Burma slab, identified for the first time here, is formed by the *Chaman slab* to the west of India (CS; Figure 5,7), dipping westward below the Helmand Block and Chaman Fault of Afghanistan and Pakistan. The Chaman slab may still be connected to the western margin of India and is imaged down to a depth of ~500-600 km (Figure 5,7).

The Chaman slab is separated from and offset northward relative to the *Makran slab* (MK; Figure 5,7). Even though subduction below the Makran and the resulting formation of the major Makran

accretionary prism is well-known (Byrne et al., 1992; Kopp et al., 2000; Yamini-Fard et al., 2007), seismic tomographic images of the Makran slab are rare. Hafkenscheid et al. (2006) showed one cross section in the western Makran that reveals an upper mantle slab that is decoupled from deeper, lower mantle anomalies, but did not explicitly identify this anomaly as a slab, which we do here, to our knowledge. The Makran slab is bounded in the east by the Owen Fracture Zone-Dalrymple Trough transform-dominated India-Arabia plate boundary that towards the north splits into the Chaman Fault and Sulaiman Ranges thrust belt (Rodriguez et al., 2014). To the east, the Makran slab is bounded by the Zagros collision zone where slabs have mostly detached from Arabia (Agard et al., 2011). The Makran slab consists of Cretaceous ocean floor that is contiguous with the Oman ophiolites that obducted onto the NE Arabian margin to the southwest (Ninkabou et al., 2021). The Makran slab reaches a depth of 650 km and appears to be detached from deeper anomalies that lie directly beneath in the lower mantle (Figure 5,6) which are part of the Mesopotamia slab identified by van der Meer et al. (2010; 2018) and Agard et al. (2011a), interpreted to result from Mesozoic subduction below the southern Eurasian margin in Iran. The Makran slab is hence representing Arabian plate lithosphere, to the west of the Indian plate.

To the south of the Makran slab, and to the south of the India slab, the *Carlsberg slab* is located at a depth of 800-1400 km (CB; Figure5), identified by Gaina et al. (2015). This is an NNE-SSW trending anomaly, striking near-orthogonal to the main trend of the India slab, and in the mantle reference frame, it is located below the late Cretaceous India-Arabia plate boundary. At this plate boundary, a series of ophiolites were obducted that reveal evidence for west-dipping Indian lithosphere subduction between ~70 and ~50 Ma, and Indian Ocean reconstructions reveal that in this time interval oblique India-Arabia motion was associated with a convergent component of ~1000 km (Gaina et al., 2015; Gnos et al., 1998; van Hinsbergen et al., 2019). Gaina et al. (2015) thus interpreted the Carlsberg slab to have consumed oceanic lithosphere of the west Indian margin that was once located west of the modern Sulaiman ranges.

The only slab that has so far been interpreted as Mesotethys-derived is the *Nepal slab* (NP; Figure 6), that is located in the depth range of 1500 – 2200 km in the lower mantle below the Himalaya. The slab is NW-SE trending and south-dipping. Van Der Voo et al. (1999), van der Meer et al. (2018), and Parsons et al. (2020) interpreted this anomaly as Mesotethyan, subducted during northward subduction below Qiangtang during the closure of the Bangong-Nujiang Ocean until Early Cretaceous.

Located to the south of the India slab is the *Maldives anomaly*, a NW-SE trending slab that is located beneath the north-western Indian Ocean, between ~1200 and 2200 km depth (Figure 6). This slab was first identified by van der Voo et al. (1999) and was interpreted to reflect Neotethyan subduction at an intra-oceanic subduction zone that had been interpreted to explain the geological record of the Kohistan arc of Pakistan, as well as ophiolites of the Zagros and Himalayan orogens (Tapponnier

et al., 1981). This interpretation was later also adopted by van der Meer et al. (2010) and van Hinsbergen et al. (2012) citing geological arguments for a Cretaceous obduction of ophiolites onto the Himalayas based on sedimentological and paleomagnetic interpretations (Abrajevitch et al., 2005; Corfield et al., 2005). Hafkenscheid et al. (2006) compared slab volumes with plate reconstructions and found that the India and Maldives slab together correspond to a larger volume than expected from solely India-Asia convergence. Assuming that all anomalies below India are Neotethyan, they explained the excess volume by interpreting that the Maldives anomaly connects to the deep part of the India anomaly and has a flat-lying portion from $\sim 20^{\circ}\text{S}$ to the equator that resulted from Cretaceous roll-back that would have opened a back-arc basin along the south Tibetan margin, a scenario like Kapp and DeCelles (2019). Closure of the back-arc basin then explains the excess volume of the combined India-Maldives slab. By the time van der Meer et al. (2018) made their compilation, new sedimentological and paleomagnetic data from the Himalayas and Indus-Yarlung ophiolites, as well as new explanations for the older data of Abrajevitch et al. (2005) and Corfield et al. (2005) had been presented. These showed that obduction of ophiolites onto the northern Indian margin occurred shortly before collision with Asia, in Eocene time (Garzanti & Hu, 2015; W. Huang et al., 2015). Van der Meer et al. (2018) thus no longer interpreted the Maldives slab as Neotethyan, although they offered no alternative interpretation. Parsons et al. (2020) recently argued again that the Maldives slab requires a Cretaceous equatorial subduction zone, but their interpretation also relied on the assumption that the Maldives slab is of Neotethyan origin. We will return to the paleogeographic interpretation of the Maldives slab in the discussion section. We note that the Maldives slab has been defined based on its shallowest portion: the deeper portions of the slab are flat-lying and reach as far south as the equator, or beyond (Figure 6).

The deepest anomalies in the mantle below India and Tibet represent the *Central China slab* (CC; Figure 6) which connects to an anomaly that covers much of the core-mantle boundary below the Indian ocean that we here identify as the *Sri Lanka slab* (SR; Figure 6). The Central China slab is a south-dipping slab that is in the lower mantle from ~ 1500 km depth to the base of the mantle. It was originally included in the Mongol-Kazakh slab (van der Meer et al., 2018), interpreted as the relics of the Mongol-Okhotsk ocean (Van Der Voo et al., 1999) that intervened North China and Siberia until the latest Jurassic (Van Der Voo et al., 2015), but it was later interpreted as a separate anomaly by van der Meer et al. (2018), who considered it possible that the slab is related to the latest Triassic closure of the Paleotethys ocean between the Qiangtang and NE Tibetan terranes. The Sri Lanka slab is found horizontally draping the core-mantle boundary below the Indian ocean and continent and Tibet (Figure 6,8).

4. Discussion

4.1 Paleotethyan and Mesotethyan slabs below India and Tibet

To analyse the plate kinematic context of slab detachment during ongoing trench and plate motion, we aim to identify the slabs that unequivocally detached from the Indian plate, and whose geological records are hence located in the Himalayas or southern Tibet. Previous tomographic analyses all assumed that each slab located below India and Tibet to the south of the Indus-Yarlung suture reflect Neotethyan lithosphere and we therefore first assess where remains of the Triassic-Early Cretaceous Mesotethyan subduction and Permo-Triassic Paleotethyan subduction may reside.

Geological evidence shows that subduction during Paleotethys and Mesotethys closure occurred both northward, below blocks that already accreted to the Tibetan margin, at mantle-stationary trenches, as well as southward and retreating during the northward motion of the migrating Qiangtang (during Paleotethys closure) and Lhasa terranes (during Mesotethys closure). Hence, in both instances, slab walls may have formed below the northern, Tibetan margin, and flat-lying slabs covering a few thousand km to the south of these walls.

The Sri Lanka slab overlying the core-mantle boundary is a clear candidate to represent the Paleotethys lithosphere that was consumed by southward subduction below the Qiangtang terrane during its northward flight to Eurasia. The Sri Lanka slab connects to the steeply dipping Central China slab that could represent the last parts of the southward subducted Paleotethyan lithosphere which have not reached the core-mantle boundary yet. Additionally, northward subducted Paleotethyan lithosphere could be contained in the ‘slab graveyard’ at the core-mantle boundary to the north of the Central China slab. Alternatively, the Central China anomaly may contain both north- and southward subducted lithosphere. The global correlations of slabs and geological records of van der Meer et al. (2018) suggests that slab walls, subducted at stable trenches, tend to sink into the lower mantle without the delay that flat-lying slabs, which subducted at migrating trenches, experience. But if subduction of the Paleotethys oceanic lithosphere was indeed double-sided, the final collision would have been a soft docking, since no slab pulls one continent below the other, and an upright folded lithosphere like the Molucca Sea slabs today (Hall & Spakman, 2015) would ‘detach’ from the surface. We speculate that such vertically arched ‘slab folds’ may sink slower than a single detached slab as sub-slab mantle under the slab-arch geometry needs to be removed sideways which could explain the still upright portion of the Central China slab.

The only slab that has thus far been interpreted as Mesotethys-derived is the Nepal slab (Figure 5,6). This slab is less than 1000 km in vertical extent, and appears much less thickened than e.g., the India slab. Because the width of the Mesotethys Ocean was like the Paleo- and Neotethys, it is unlikely that the Nepal slab contains all Mesotethys lithosphere. The evidence for Triassic to early Cretaceous subduction below the Lhasa terrane, e.g. in the form of arc magmatic rocks (Kapp &

Decelles, 2019; S. Li et al., 2019), moreover, suggests that there was subduction of lithosphere below the Lhasa terrane throughout its northward flight towards Eurasia. Kapp & Decelles (2019) suggested this was Neothethyan lithosphere subducting northward since the Triassic. We consider this unlikely: paleomagnetic data place Lhasa against the northern Gondwana margin in the late Triassic (Li et al., 2016), followed by Neotethys opening until the early Cretaceous. In this view, a south-directed subduction zone as suggested by Zhu et al. (2015), would be more likely. Either way, a flat-lying slab is expected of similar magnitude as that of the Paleotethys (overturned if subducted northward, normal facing if subducted southward) at a shallower position in the mantle. We infer that the Nepal slab is the northern tip of a flat-lying slab that continues southward until near-equatorial latitudes and includes (at least part of) the Maldives slab (Figure 5,6). This interpretation assigns a similar dimension to the Mesotethys and Paleotethys-derived slabs as dictated by plate tectonic reconstructions. Below the massive slab wall of the India slab, this horizontal slab Nepal-Maldives slab would then be bent down under the likely faster sinking India slab wall (Figure8). The Nepal slab may then represent the remnants of an arched slab ‘fold’.

Realizing that a large part of the mid-mantle anomalies below India may be Mesotethyan lithosphere rather than Neotethyan makes interpreting the Maldives slab as Neotethys not a necessity. As outlined above, there is no conclusive geological evidence that a slab detached at an equatorial intra-oceanic subduction zone upon arrival of the northern Indian margin in the trench. Parsons et al. (2020) recently concluded that the Maldives slab is the conclusive evidence to this end, but this argument relied on the assumption that all sub-Indian plate anomalies are Neotethyan. Tomographic evidence does not exclude an equatorial subduction zone, since the shallower part of the Maldives slab could be a separate anomaly that lies on top of a flat-lying Mesotethys slab. However, an intra-oceanic equatorial subduction zone is not required by the tomographic model. Below, we focus our analysis on the anomalies whose Neotethyan affinity is undisputed. This includes the India, Himalaya, Carlsberg, Hindu Kush, Burma, and Chaman slabs and the horizontally underthrust Indian lithosphere below Tibet.

4.2 Timing of Neotethyan slab detachment events

Of the youngest slabs that consumed Indian plate lithosphere, the Chaman and Burma slabs are still connected to the Indian plate, the Hindu Kush slab is in the process of breaking off (Kufner et al., 2021), and the Himalaya, Carlsberg, and India slabs are detached. We first evaluate when this detachment occurred, then evaluate the kinematic setting in which detachment occurred, and finally briefly evaluate the potential to detect geological signatures of this detachment from Himalayan geology.

We estimate of the timing of detachment of the Himalayas through kinematic restoration of the timing and duration of horizontal Indian underthrusting below Tibet. Kinematic reconstructions of India-Asia convergence combined with reconstruction of Tibetan shortening (van Hinsbergen et al., 2019) shows that the modern northern margin of the underthrust Indian plate lithosphere imaged by seismological data (Agius & Lebedev, 2013; Chen et al., 2017; van Hinsbergen et al., 2019) underthrusts below the Himalayas thrust front around 30-25 Ma at the syntaxes, becoming progressively younger towards the central-eastern Himalayas to around 15-13 Ma. This suggests that the Himalayas slab detached diachronously, starting around 25 Ma at the western and eastern syntaxes and progressively migrating inwards towards the central-eastern part of the plate boundary around 15 Ma (van Hinsbergen et al., 2019). Or, alternatively, detachment may have occurred at a deeper level, after which the remaining Indian lithosphere rebounded back to a horizontal position (Magni et al., 2017), although with the continued northward advance below Tibet, an inclined Indian margin would have acted as a plow (Hinsbergen et al., 2020) which could have prevented such a rebound. When viewed in a mantle frame of reference (Dobrovine et al., 2012), the reconstruction of van Hinsbergen et al. (2019) places the Himalayas thrust front above the modern position of the Himalayas slab. We therefore favour an interpretation that detachment of the Himalayas slab coincided with the base of the continental Indian lithosphere and that this lithosphere horizontally underthrusts Tibet.

The Hindu Kush slab in the west must represent a lateral equivalent of the Himalayas slab that escaped Miocene detachment, or, more likely, where detachment occurred at a deeper level. The Hindu Kush slab is ~600 km long and is offset southward from the northernmost part of the underthrust Indian lithosphere below the Pamir by ~300 km (Figure 5). Hence, when detachment of the Himalayas slab from the westernmost Indian lithosphere now below the Pamir crust occurred around 25 Ma, about 300 km of the Hindu Kush slab was likely still located at the surface adjacent to India's northwestern margin, but the remaining deepest 300 km of the Hindu Kush lithosphere had already subducted then. The volume of the Himalayas slab suggests it contains more than 300 km of subducted lithosphere and is thus not a detached equivalent of the Hindu Kush slab: detachment of the Himalayas slab more likely removed a deeper part of the Hindu Kush slab and detached at a greater depth, of up to some 300 km, than at the north Indian continental margin where it detached at the depth of the base of the lithosphere.

Estimating the timing of decoupling between the Himalayas and India slabs is more challenging. The Himalayas slab is ~500 km long and depending on the assumed amount of thickening may contain two or three times that length in lithosphere. Comparing this with estimates of India-Asia convergence suggests that the Himalayas slab contains lithosphere that subducted sometime between ~40-35 Ma and 25-15 Ma (Replumaz et al., 2010). Hence, if detachment occurred at shallow depth, it would have occurred around 40-35 Ma. However, if detachment occurred at

greater depth, e.g. around 300 km as argued above for the Hindu Kush slab, detachment occurred later, after at least part of the Himalayas slab had already been subducted.

The Carlsberg slab in the west was interpreted to contain lithosphere that subducted during highly oblique convergence between India and Arabia, between the Maastrichtian onset of subduction recorded by ophiolites in the Sulaiman ranges (Gaina et al., 2015; Gnos et al., 1998). Upper Paleocene to lower Eocene clastics in the Sulaiman ranges with ophiolite detritus (Khan & Clyde, 2013) show that obduction was underway by 60-55 Ma, and arrest of convergence and final emplacement was estimated at ~50 Ma (Gaina et al., 2015; Gnos et al., 1998). When placed in a mantle frame of reference (Dobrovine et al., 2012), the west Indian margin at 50 Ma is located above the Carlsberg slab. Moreover, reconstructions of India-Arabia motion using Indian ocean basin reconstructions (DeMets & Merkouriev, 2021; Gaina et al., 2015) reveal that post-50 Ma India-Helmand convergence at the latitude of the Chaman slab was associated with an E-W component of convergence of ~500-600 km (alongside a much larger component of left-lateral strike-slip motion) coincident with the Chaman slab length. A 50 Ma detachment age of the Carlsberg slab thus seems a reasonable estimate.

4.3 Slab detachment during ongoing convergence: concept and future study areas

The plate kinematic history during which modern mantle structure evolved, reveals that despite ongoing plate convergence and absolute northward motion of the Indian plate and the plate boundary along southern Tibet, multiple slab detachment events occurred. An important corollary of this history is that commonly assumed geodynamic conditions used to simulate slab detachment in numerical and analogue experiments – an arrest of plate convergence, and a mantle-stationary trench – did not apply when the slabs detached from subducting Indian plate lithosphere. Two first-order differences between model predictions and the reconstructed history of slab detachments from the Indian plate follow straightforwardly from our analysis above.

First, the ongoing plate convergence between India and Asia implies that there cannot have been a long delay time between subduction and detachment of a slab. Model predictions suggest that slabs break-off 5-30 Ma after their subduction following a phase of gradual shearing and viscous necking (Andrews & Billen, 2009; Bercovici & Skemer, 2017; Duretz et al., 2012; Gerya et al., 2004; Royden, 1993). Plate convergence rates in the last 45 Ma have varied from 4-8 cm/a (DeMets & Merkouriev, 2021) of which no more than ~2 cm/a was accommodated by upper plate shortening in Tibet (van Hinsbergen et al., 2019). Hence, for every 1 Ma delay time between subduction and detachment, a potential necking zone in a slab would sink 20-60 km. After the last phase of slab detachment from the northern Indian margin, no detectable slab has formed and the horizontal offset between the north Indian margin imaged below Tibet and the Himalayas slab shows that detachment

must have occurred quickly (within a few Ma) after arrival of that margin at the trench, and at a shallow depth around the base of the lithosphere.

Second, detachment was probably not only caused by vertical stretching of lithosphere. The Carlsberg slab was subducting westwards while India moved northwards: it is inevitable that this slab was dragged sideways through the mantle during its subduction, and during the arrival of the Indian continental lithosphere in the trench. At present, lateral slab dragging occurs with the Chaman and Burma slabs (Figure 7), and has also been shown for the Tonga-Kermadec and Gibraltar slabs (van de Lagemaat et al., 2018; Spakman et al., 2018; Parsons et al., 2021). This dragging of the Carlsberg slab must have been resisted by the ambient mantle leading to a slab-strike parallel resistive shear traction (Spakman et al. 2018) that may have aided break-off as this viscous coupling between slab and mantle may cause large slab-strike parallel deformation (Giardini and Woodhouse 1986; Chertova et al. 2018). Such northward dragging not only applies to the slabs on the west and east side of India, but also follows from our analysis of the Hindu Kush slab. The slab is currently located ~300 km to the south of the northern edge of the Indian plate located below the Pamir (Figure 5), and this may reflect that the slab retreated relative to India over this distance since the detachment of the Himalayas slab from India's northwestern margin some 25-30 Ma ago (cf. the 3D convergence-detachment model of Duretz et al. 2014). But in that same time period, the Indian plate moved >1000 km northward. The Hindu Kush slab must thus have been dragged northward over some 700 km through the mantle in the last ~25 Ma, consistent with its offset relative to the Himalayas slab. Such a history of northward advance also applies to the Himalayas slab given its overturned orientation. Hence, the ongoing absolute motion of the Indian plate adds an oppositely directed force on the slab as mantle material must be removed in front of the slab to accommodate forward slab transport. This forcing may localize where the slab is weakest which is classically the slab bending zone below the trench but may also occur deeper due to subducted lithosphere weakness (Gerya et al., 2021). In this scenario, the slab can be sheared-off shallowly, i.e., near the base of the lithosphere of the downgoing plate (Figure 9) which contrasts with the lithosphere-age dependent detachment depth inferred from previous modelling.

The question then arises whether slab detachment during ongoing plate motion and trench advance yields geological signatures that are like the vertical necking that is portrayed in classical experiments. The detailed earthquake hypocenter studies in the Hindu Kush slab of Kufner et al. (2017; 2021) elegantly show that the shear zone along which detachment is occurring mimics the predicted shear zones by vertical necking experiments (Duretz et al., 2011), even though the Hindu Kush slab is being dragged northward. On the other hand, with ongoing absolute plate motion of the downgoing plate, a detachment zone is immediately being overridden. The classically suggested high-temperature pulse that was inferred to cause magmatism or metamorphism in a suture zone (van de Zedde and Wortel, 2001), may therefore not be recorded in the collision zone.

To determine the geological effects of slab detachment during ongoing plate and trench migration and to evaluate whether there is dependence of geological signatures on the absolute plate motion direction relative to slab strike, calls for future numerical and analogue experiments in combination with field testing. To determine the effects of near slab-strike parallel dragging, we identify the Chaman and Burma slabs as key candidates for the study of present-day geophysical expressions. Effects on the longer geological evolution associated with detachment associated with slab-strike parallel dragging may be contained in the Eocene geological record of the Sulaiman Ranges of Pakistan.

The highly detailed studies of Kufner et al. (2016; 2017; 2021) of the Hindu Kush slab provide key constraints for detachment during slab-strike perpendicular dragging. The Miocene geological record of the Himalayas would provide a longer-term geological perspective on the effects of slab detachment during plate motion. In that light, the study of Webb et al. (2017) is intriguing: Those authors interpreted an evolution of slab detachment below the Himalayas that started in the syntaxes around 30-25 Ma and progressed to the central-eastern Himalayas until ~13 Ma. They concluded an identical timing and asymmetry in detachment age as we infer from the shape of the horizontally underthrust northern Indian margin below Tibet (Figure 5,6,7), but based this on an entirely independent data set and line of argumentation. Their study was based on along-strike studies of the Himalayas and southern Tibet and identified trends in high-K and adakitic magmatism and geochronological estimates of major ductile faults in the orogen. The study of Webb et al. (2017), but also earlier studies arguing for a ~25 Ma onset for changing thermal conditions in the collision zone (Maheo et al., 2002), may thus provide an excellent starting point for hypothesis building as basis for numerical and analogue experiments of slab detachment during ongoing plate convergence and trench motion.

Also, the recent unprecedented high-resolution India-Asia convergence records of DeMets and Merkouriev (2021) provide key information. During the inferred detachment period between ~30-25 and 13 Ma they showed a subtle slow-down in plate convergence rates and following 13 Ma a steady rate of ~4 cm/a. Intriguingly, India-Asia convergence accelerated by a few cm/a between 40 and 30 Ma, around which time the detachment of the Himalayas slab from the India slab may have occurred. This detachment would have potentially removed the mantle resistance against northward slab dragging removing, at least temporarily, this control on the northward motion of the Indian plate, but also this speculation requires future dynamic analysis.

Finally, we note that the initial India-Asia collision recorded in the Tibetan Himalayas around 60-50 Ma (An et al., 2021; Najman et al., 2010) is widely interpreted to be followed by slab detachment along the Indian continental margin under the assumption that this collision represented the arrival of the contiguous Indian continent at the Tibetan trench (Kohn et al., 2002; H. Lee et al., 2009; Zhu et al., 2015). If there was slab detachment in the late Paleocene or early Eocene, it is not detectable within the India anomaly. We note that Indian plate subduction rates in this time period were in excess of 150

km/Ma (DeMets & Merkouriev, 2021; van Hinsbergen et al., 2019): even if slab detachment occurred in this time period, it could have taken only a few Ma for a slab to reach to the base of the upper mantle again and it is questionable whether there would have been any detectable dynamic or geological response. The kinematic restoration of van Hinsbergen et al. (2012; 2019) interpreted the Paleocene-early Eocene collision reconstructed from the northern Himalayas as recording the arrival of a microcontinent at the southern Eurasian margin and interpreted the modern northern margin of India underthrust below Tibet as the former passive margin of northern India that only arrived at the southern Himalayan margin in the Miocene. Subduction of microcontinental lithosphere without slab detachment is common in Tethyan mountain belts (van Hinsbergen and Schouten, 2021) and this scenario would suggest that detachment of the Himalayas slab occurred along the passive continental margin, as commonly inferred in slab detachment models. If all lithosphere that subducted in the Himalayas after the early Eocene (Hu et al., 2016; Ingalls et al., 2016; Replumaz et al., 2010) or late Eocene (Aitchison et al., 2007; Jagoutz et al., 2015; Martin et al., 2020) was continental, as more commonly assumed, the timing, causes, and locations of slab break-off within continental lithosphere following 1000 km or more of rapid continental subduction, remain to be explained.

5. Conclusions

Slab detachment is a key process in the plate tectonic cycle and may have profound impact on the geological record of orogens causing metamorphism, magmatism, economic mineralization, and surface uplift, and may be associated with plate reorganizations. Conceptual, numerical, and analogue models that aim to find the dynamic link between slab detachment and these geological observations assume that plate convergence stops prior to detachment, that the slab and trench remain mantle-stationary for 10 Ma or more, and that slab detachment is then a gradual and laterally diachronous process. However, plate convergence typically continues, and trenches are rarely mantle-stationary during slab detachment. In this paper, we investigate the history of slab detachments from the Indian plate to develop a kinematic framework for slab detachment during ongoing absolute plate and trench motion. Seismic tomography has long shown that no major slabs are currently attached to the Indian plate below the Himalaya, and major anomalies located in the upper and lower mantle below India have widely been interpreted as detached relict slabs. All these slabs are located far south of the modern northern margin of the Indian continent that is seismically imaged to horizontally underthrust the Tibetan Plateau. The offset between the slabs and the margin from which they detached is consistent with the kinematic evidence that India's absolute plate motion continued throughout the Cenozoic until the present day.

To identify which slabs must have broken off the fast-moving Indian plate, we first update the correlation of subducted slabs below India and Tibet to lithosphere that subducted in Mesozoic-

Cenozoic time. The slabs below India were among the first identified following the advent of global tomography and were initially all assumed to represent Neotethyan lithosphere. Because their volume far exceeds volumes predicted from India-Asia convergence reconstructions, intra-oceanic subduction was inferred within the Neotethyan realm. But global correlations have shown that slabs that subducted in Permo-Triassic and Jurassic time are generally also still imaged in the lower mantle. In the case of the mantle beneath the Indian plate, slabs that comprise of the Mesotethys that subducted in Late Triassic-Early Cretaceous time and Paleotethys (Permian - Late Triassic) oceanic lithosphere should still be visible. We use first-order estimates of expected slab shape and length to infer that a Paleotethyan derived slab (here named Sri Lanka slab) is located at the base of the mantle and may include part of the previously identified Central China slab below northern Tibet. A Mesotethyan slab horizontally underlies the India slab wall in the mid-mantle and includes the previously identified Maldives and Nepal anomalies. Whereas tomography does not exclude that an equatorial Neotethyan slab may have formed, such an interpretation is not required to explain the tomography. Only of the India, Carlsberg, and Himalayas slabs we are confident that they must represent Neotethyan lithosphere that detached from the Indian plate. The India and Himalayas slabs detached from the northern plate margin, the Carlsberg slab from the western margin. In addition, the Hindu Kush, Burma, and the newly identified Chaman slabs are still attached to India.

We identify that the three detached Neotethyan slabs (India, Carlsberg, Himalayas slabs) detached during ongoing northward motion of India relative to the mantle. During their detachment, they were not passively dangling in the mantle during which time gradual necking would lead to detachment, but we hypothesize that in addition to slab pull the resistance of the mantle against forward slab dragging of laterally wide slabs may have played a key role. We discuss that slab detachment during ongoing plate motion may have different geological expressions than inferred from previous detachment modelling, and that these may differ as function of slab strike relative to absolute plate motion direction. Slabs to the west (Chaman) and east (Burma) of India are dragged near slab-strike parallel through the mantle, and detachment under those circumstances must have affected the older, deeper, Carlsberg slab as well. The latter slab likely detached in Eocene time, and we identify the Sulaiman Ranges of west Pakistan as key area to test possible signatures (Figure 10).

Slabs at the northern extent of the Indian plate detached following and during slab advance. This is illustrated by the northward overturned Himalayas slab that was the last to detach. An entirely independent, previously published estimate of the last phase of slab detachment using magmatism and exhumation patterns in the Himalayas coincides with our estimate of the last phase of detachment on kinematic restoration of horizontally underthrust northern Indian margin below Tibet and may provide a geological record to calibrate the geological effects of detachment during ongoing downward plate motion. In addition, the well-documented active detachment in the Hindu Kush slab, which we show was dragged through the mantle over a distance close to 700 km in the Cenozoic, may provide a

geophysical record of detachment of a forwardly dragged slab. Our analysis thus provides new conditions for slab detachment to occur in the geodynamic context of ongoing relative and absolute plate motions, which may be used by numerical and analogue experiments to evaluate geological signatures of this key geodynamic process.

Acknowledgements

AQ, NL, and DJJvH acknowledge funding through Netherlands Organization for Scientific Research (NWO) Vici grant 865.17.001 to DJJvH.

References

- Abrajevitch, A. V, Ali, J. R., Aitchison, J. C., Davis, A. M., Liu, J., & Ziabrev, S. V. (2005). Neotethys and the India – Asia collision : Insights from a palaeomagnetic study of the Dazhuqu ophiolite , southern Tibet, 233, 87–102. <https://doi.org/10.1016/j.epsl.2005.02.003>
- Agard, P., Omrani, J., Jolivet, L., Whitechurch, H., Vrielynck, B., Spakman, W., et al. (2011a). Zagros orogeny: A subduction-dominated process. *Geological Magazine*, 148(5–6), 692–725. <https://doi.org/10.1017/S001675681100046X>
- Agard, P., Omrani, J., Jolivet, L., Whitechurch, H., Vrielynck, B., Spakman, W., et al. (2011b). Zagros orogeny: A subduction-dominated process. *Geological Magazine*, 148(5–6), 692–725. <https://doi.org/10.1017/S001675681100046X>
- Agius, M. R., & Lebedev, S. (2013). Tibetan and Indian lithospheres in the upper mantle beneath Tibet: Evidence from broadband surface-wave dispersion. *Geochemistry, Geophysics, Geosystems*, 14(10), 4260–4281. <https://doi.org/10.1002/ggge.20274>
- Aitchison, J. C., Ali, J. R., & Davis, A. M. (2007). When and where did India and Asia collide ? *Journal of Geophysical Research*, 112(November 2006), 1–19. <https://doi.org/10.1029/2006JB004706>
- Amaru, M. (2007). *Global travel time tomography with 3-D reference models. Geologica Ultraiectina* (Vol. 274).
- Andrews, E. R., & Billen, M. I. (2009). Rheologic controls on the dynamics of slab detachment. *Tectonophysics*, 464(1–4), 60–69. <https://doi.org/10.1016/j.tecto.2007.09.004>

773 Atherton, M. P., & Ghani, A. A. (2002). Slab breakoff: a model for Caledonian , Late Granite syn-
774 collisional magmatism in the orthotectonic (metamorphic) zone of Scotland and Donegal ,
775 Ireland. *LITHOS*, 62, 65–85.

776 Běhouňková, M., & Čížková, H. (2008). Long-wavelength character of subducted slabs in the lower
777 mantle. *Earth and Planetary Science Letters*, 275, 43–53.
778 <https://doi.org/10.1016/j.epsl.2008.07.059>

779 Bercovici, D., & Skemer, P. (2017). Grain damage , phase mixing and plate-boundary formation.
780 *Journal of Geodynamics*, 108(April), 40–55. <https://doi.org/10.1016/j.jog.2017.05.002>

781 Bercovici, D., Schubert, G., & Ricard, Y. (2015). Abrupt tectonics and rapid slab detachment with
782 grain damage. *PNAS*, 112(5). <https://doi.org/10.1073/pnas.1415473112>

783 Bijwaard, H., Spakman, W., & Engdahl, E. R. (1998). Closing the gap between regional and global
784 travel time tomography. *Journal of Geophysical Research: Solid Earth*, 103(B12), 30055–
785 30078. <https://doi.org/10.1029/98jb02467>

786 Billen, M. I. (2010). Slab dynamics in the transition zone. *Physics of the Earth and Planetary*
787 *Interiors*, 183, 296–308. <https://doi.org/10.1016/j.pepi.2010.05.005>

788 Boschman, L. M., van Hinsbergen, D. J. J., Kimbrough, D. L., Langereis, C. G., & Spakman, W.
789 (2018). The Dynamic History of 220 Million Years of Subduction Below Mexico: A Correlation
790 Between Slab Geometry and Overriding Plate Deformation Based on Geology, Paleomagnetism,
791 and Seismic Tomography. *Geochemistry, Geophysics, Geosystems*, 19(12), 4649–4672.
792 <https://doi.org/10.1029/2018GC007739>

793 Buiter, S. J. H., & Pfiffner, O. A. (2003). Numerical models of the inversion of half-graben basins,
794 22(5), 1–16. <https://doi.org/10.1029/2002TC001417>

795 Buiter, S. J. H., Govers, R., & Wortel, M. J. R. (2002). Two-dimensional simulations of surface
796 deformation caused by slab detachment, 354, 195–210.

797 Burke, K., Steinberger, B., Torsvik, T. H., & Smethurst, M. A. (2008). Plume Generation Zones at the
798 margins of Large Low Shear Velocity Provinces on the core – mantle boundary, 265, 49–60.
799 <https://doi.org/10.1016/j.epsl.2007.09.042>

800 Butterworth, N. P., Talsma, A. S., Müller, R. D., Seton, M., Bunge, H. P., Schuberth, B. S. A., et al.
801 (2014). Geological, tomographic, kinematic and geodynamic constraints on the dynamics of
802 sinking slabs. *Journal of Geodynamics*, 73, 1–13. <https://doi.org/10.1016/j.jog.2013.10.006>

803 Byrne, D. E., Sykes, L. R., & Davis, D. A. N. M. (1992). Great Thrust Earthquakes and Aseismic Slip
804 Along the Plate Boundary of the Makran motion in the form of earthquakes may occur in a

805 variety (e . g ., southern Chile), while still others have experienced no of ways at subduction
806 zones . Some margins produ. *Journal of Geop*, 97(91), 449–478.

807 Chemenda, A. I., Mattauer, M., Malavieille, J., & Bokun, A. N. (1995). normal faulting : Results from
808 physical modelling. *Earth and Planetary Science Letters*, 132, 225–232.

809 Chen, M., Niu, F., Tromp, J., Lenardic, A., Lee, C. A., Cao, W., & Ribeiro, J. (2017). Lithospheric
810 foundering and underthrusting imaged beneath Tibet. *Nature Communications*, 8, 1–10.
811 <https://doi.org/10.1038/ncomms15659>

812 Conrad, C. P., & Lithgow-Bertelloni, C. (2002). How mantle slabs drive plate tectonics. *Science*,
813 298(5591), 207–209. <https://doi.org/10.1126/science.1074161>

814 Copley, A., Avouac, J. P., & Royer, J. Y. (2010). India-Asia collision and the Cenozoic slowdown of
815 the Indian plate: Implications for the forces driving plate motions. *Journal of Geophysical*
816 *Research: Solid Earth*, 115(3), 1–14. <https://doi.org/10.1029/2009JB006634>

817 Corfield, R. ., Watts, A. ., & Searle, M. . (2005). Subsidence history of the north Indian continental
818 margin , Zaskar – Ladakh. *Journal Ofthe Geological Society, London*, 162(1991), 135–146.

819 Le Dain, Y. A., Topponnier, P., & Molnar, P. (1984). Active Faulting And Tectonics Of Burma And
820 Surrounding Regions. *Journal of Geophysical Research*, 89(Figure 1), 453–472.

821 Davies, J. H., & von Blanckenburg, F. (1995). Slab breakoff: A model of lithosphere detachment and
822 its test in the magmatism and deformation of collisional orogens. *Earth and Planetary Science*
823 *Letters*, 129(1–4), 85–102. [https://doi.org/10.1016/0012-821X\(94\)00237-S](https://doi.org/10.1016/0012-821X(94)00237-S)

824 DeMets, C., & Merkouriev, S. (2021). Detailed reconstructions of India-Somalia plate motion, 60 Ma
825 to present: Implications for Somalia plate absolute motion and India-Eurasia plate motion.
826 *Geophysical Journal International*, 1730–1767. <https://doi.org/10.1093/gji/ggab295>

827 Domeier, M., Doubrovine, P. V., Torsvik, T. H., Spakman, W., & Bull, A. L. (2016). Global
828 correlation of lower mantle structure and past subduction. *Geophysical Research Letters*, 43(10),
829 4945–4953. <https://doi.org/10.1002/2016GL068827>

830 Doubrovine, P. V., Steinberger, B., & Torsvik, T. H. (2012). Absolute plate motions in a reference
831 frame defined by moving hot spots in the Pacific , Atlantic , and Indian oceans. *Journal of*
832 *Geophysical Research*, 117(July), 1–30. <https://doi.org/10.1029/2011JB009072>

833 Duretz, Gerya, T. V., & May, D. A. (2011). Numerical modelling of spontaneous slab breakoff and
834 subsequent topographic response. *Tectonophysics*, 502(1–2), 244–256.
835 <https://doi.org/10.1016/j.tecto.2010.05.024>

836 Duretz, T., Schmalholz, S. M., & Gerya, T. V. (2012). Dynamics of slab detachment. *Geochemistry*

- 837 *Geophysics Geosystems*, 13(3). <https://doi.org/10.1029/2011GC004024>
- 838 Duretz, T., Gerya, T. V., & Spakman, W. (2014). Slab detachment in laterally varying subduction
839 zones: 3-D numerical modeling. *Geophysical Research Letters*, 41(6), 1951–1956.
840 <https://doi.org/10.1002/2014GL059472>
- 841 Ely, K. S., & Sandiford, M. (2010). Seismic response to slab rupture and variation in lithospheric
842 structure beneath the Savu Sea, Indonesia. *Tectonophysics*, 483(1–2), 112–124.
843 <https://doi.org/10.1016/j.tecto.2009.08.027>
- 844 Fernández-garcía, C., Guillaume, B., & Brun, J. (2019). Tectonophysics 3D slab break off in
845 laboratory experiments. *Tectonophysics*, 773(October), 1–11.
846 <https://doi.org/10.1016/j.tecto.2019.228223>
- 847 Forsyth, D., & Uyedat, S. (1975). On the Relative Importance of the Driving Forces of Plate Motion.
848 *Geophysical Journal of the Royal Astronomical Society*, 43(1), 163–200.
849 <https://doi.org/10.1111/j.1365-246X.1975.tb00631.x>
- 850 Fukao, Y., Obayashi, M., Inoue, H., & Nenbai, M. (1992). Subducting Slabs Stagnant in the Mantle
851 Transition Zone. *Journal of Geophysical Research*, 97, 4809–4822.
- 852 Fukao, Y., Widiyantoro, S., & Obayashi, M. (2001). Stagnant slabs in the upper and lower mantle
853 transition region, (1999), 291–323.
- 854 Gaina, C., Douwe, J. . van H., & Spakman, W. (2015). Tectonic interactions between India and
855 Arabia since the Jurassic reconstructed from marine geophysics, ophiolite geology, and seismic
856 tomography. *Tectonics*, 34, 875–906. <https://doi.org/10.1002/2014TC003780>.Received
- 857 Garzanti, E., & Hu, X. (2015). Latest Cretaceous Himalayan tectonics : Obduction , collision or
858 Deccan-related uplift ? *Gondwana Research*, 28(1), 165–178.
859 <https://doi.org/10.1016/j.gr.2014.03.010>
- 860 Garzanti, E., Rade, G., & Malusà, M. G. (2018). Earth-Science Reviews Slab breakoff: A critical
861 appraisal of a geological theory as applied in space and time. *Earth Science Reviews*, 177(July
862 2017), 303–319. <https://doi.org/10.1016/j.earscirev.2017.11.012>
- 863 Gerya, T V, Bercovici, D., & Becker, T. W. (2021). Dynamic slab segmentation due to brittle –
864 ductile damage in the outer rise. *Nature*, 599(November). [https://doi.org/10.1038/s41586-021-](https://doi.org/10.1038/s41586-021-03937-x)
865 [03937-x](https://doi.org/10.1038/s41586-021-03937-x)
- 866 Gerya, Taras V., Yuen, D. A., & Maresch, W. V. (2004). Thermomechanical modelling of slab
867 detachment. *Earth and Planetary Science Letters*, 226(1–2), 101–116.
868 <https://doi.org/10.1016/j.epsl.2004.07.022>

- 869 Gnos, E., Khan, M., Mahmood, K., Khan, A. S., Shafique, N. A., & Villa, I. M. (1998). Bela oceanic
870 lithosphere assemblage and its relation to the Â union hotspot Re. *Tectonophysics*.
- 871 González, J. R., & Negredo, A. M. (2012). The role of the overriding plate thermal state on slab dip
872 variability and on the occurrence of flat subduction. *Geochemistry, Geophysics, Geosystems*,
873 13(1), 1–21. <https://doi.org/10.1029/2011GC003859>
- 874 Grand, S. P., van der hilst, R. ., & Widiyantoro, S. (1997). Global Seismic Tomography: A Snapshot
875 of Convection in the Earth. *GSA Today*, 7(4), 1–7.
- 876 Hafkenscheid, E., Wortel, M. J. R., & Spakman, W. (2006). Subduction history of the Tethyan region
877 derived from seismic tomography and tectonic reconstructions. *Journal of Geophysical*
878 *Research: Solid Earth*, 111(8), 1–26. <https://doi.org/10.1029/2005JB003791>
- 879 Hall, R., & Spakman, W. (2002). Subducted slabs beneath the eastern Indonesia-Tonga region:
880 Insights from tomography. *Earth and Planetary Science Letters*, 201(2), 321–336.
881 [https://doi.org/10.1016/S0012-821X\(02\)00705-7](https://doi.org/10.1016/S0012-821X(02)00705-7)
- 882 Hall, R., & Spakman, W. (2015). Tectonophysics Mantle structure and tectonic history of SE Asia.
883 *Tectonophysics*, 658, 14–45. <https://doi.org/10.1016/j.tecto.2015.07.003>
- 884 Hébert, R., Bezard, R., Guilmette, C., Dostal, J., Wang, C. S., & Liu, Z. F. (2012). The Indus –
885 Yarlung Zangbo ophiolites from Nanga Parbat to Namche Barwa syntaxes , southern Tibet :
886 First synthesis of petrology , geochemistry , and geochronology with incidences on geodynamic
887 reconstructions of Neo-Tethys. *Gondwana Research*, 22(2), 377–397.
888 <https://doi.org/10.1016/j.gr.2011.10.013>
- 889 Hilst, R. D. Van Der, Engdahl, R., Spakman, W., & Nolet, G. (1991). Tomographic imaging of
890 subducted lithosphere below northwest Pacific island arcs. *Nature*, 353.
- 891 Hilst, R. D. Van Der, Widiyantorot, S., & Engdahl, E. R. (1997). Evidence for deep mantle circulation
892 from global tomography. *Nature*, 386(April).
- 893 van Hinsbergen, D. J. J., Hafkenscheid, E., Spakman, W., Meulenkamp, J. ., & Wortel, R. (2005).
894 Nappe stacking resulting from subduction of oceanic and continental lithosphere below Greece.
895 *Geology*, (4), 325–328. <https://doi.org/10.1130/G20878.1>
- 896 van Hinsbergen, D. J. J., Lippert, P. C., Dupont-Nivet, G., McQuarrie, N., Doubrovine, P. V.,
897 Spakman, W., & Torsvik, T. H. (2012). Greater India Basin hypothesis and a two-stage
898 Cenozoic collision between India and Asia. *Proceedings of the National Academy of Sciences*,
899 109(20), 7659–7664. <https://doi.org/10.1073/pnas.1117262109>
- 900 van Hinsbergen, D. J. J., Lippert, P. C., Li, S., Huang, W., Advokaat, E. L., & Spakman, W. (2019).

- Tectonophysics Reconstructing Greater India : Paleogeographic , kinematic , and geodynamic perspectives. *Tectonophysics*, (May 2017), 0–1. <https://doi.org/10.1016/j.tecto.2018.04.006>
- van Hinsbergen, D. J., Steinberger, B., & Doubrovine, P. V. (2011). Acceleration and deceleration of India - Asia convergence since the Cretaceous : Roles of mantle plumes and continental collision. *Journal of Geophysical Research*, 116, 1–20. <https://doi.org/10.1029/2010JB008051>
- van Hinsbergen, Douwe J.J., Lippert, P. C., Li, S., Huang, W., Advokaat, E. L., & Spakman, W. (2019). Reconstructing Greater India: Paleogeographic, kinematic, and geodynamic perspectives. *Tectonophysics*, 760(May 2017), 69–94. <https://doi.org/10.1016/j.tecto.2018.04.006>
- van Hinsbergen, Douwe J.J., Spakman, W., de Boorder, H., van Dongen, M., Jowitt, S. M., & Mason, P. R. D. (2020). Arc-Type Magmatism Due to Continental-Edge Plowing Through Ancient Subduction-Enriched Mantle. *Geophysical Research Letters*, 47(9), 1–11. <https://doi.org/10.1029/2020GL087484>
- van Hinsbergen, Douwe J J, & Schouten, T. L. A. (2021). Deciphering paleogeography from orogenic architecture : constructing orogens in a future supercontinent as thought experiment. *American journal of science*, 321, 955–1031. <https://doi.org/10.2475/06.2021.09>
- van Hinsbergen, Douwe J J, Kapp, P., Nivet, G. D., Lippert, P. C., Decelles, P. G., & Torsvik, T. H. (2011). Restoration of Cenozoic deformation in Asia and the size of Greater India. *Tectonics*, 30, 1–31. <https://doi.org/10.1029/2011TC002908>
- Hinsbergen, Douwe J J Van, Lippert, P. C., Dupont-nivet, G., & Mcquarrie, N. (2012). Greater India Basin hypothesis and a two-stage Cenozoic collision between India and Asia, 109(20). <https://doi.org/10.1073/pnas.1117262109>
- Hodges, K. V. (2000). Tectonics of the Himalaya and Southern Tibet from two perspectives. *Bulletin of the Geological Society of America*, 112(3), 324–350. [https://doi.org/10.1130/0016-7606\(2000\)112<324:TOTHAS>2.0.CO;2](https://doi.org/10.1130/0016-7606(2000)112<324:TOTHAS>2.0.CO;2)
- Hu, X., Garzanti, E., Wang, J., Huang, W., An, W., & Webb, A. (2016). The timing of India-Asia collision onset – Facts , theories , controversies. *Earth Science Reviews*, 160, 264–299. <https://doi.org/10.1016/j.earscirev.2016.07.014>
- Huang, J., & Zhao, D. (2006). High-resolution mantle tomography of China and surrounding regions. *Journal of Geophysical Research*, 111(March), 1–21. <https://doi.org/10.1029/2005JB004066>
- Huang, W., Hinsbergen, D. J. J. Van, Maffione, M., Orme, D. A., Dupont-nivet, G., Guilmette, C., et al. (2015). Lower Cretaceous Xigaze ophiolites formed in the Gangdese forearc : Evidence from

933 paleomagnetism , sediment provenance , and stratigraphy. *Earth and Planetary Science Letters*,
934 415, 142–153. <https://doi.org/10.1016/j.epsl.2015.01.032>

935 van Hunen, J., & Allen, M. B. (2011). Continental collision and slab break-off: A comparison of 3-D
936 numerical models with observations. *Earth and Planetary Science Letters*, 302(1–2), 27–37.
937 <https://doi.org/10.1016/j.epsl.2010.11.035>

938 Ingalls, M., Rowley, D. B., Currie, B., & Colman, A. S. (2016). Large-scale subduction of continental
939 crust implied by India-Asia mass-balance calculation. *Nature Geoscience*, 9(11), 848–853.
940 <https://doi.org/10.1038/ngeo2806>

941 Jagoutz, O., Royden, L., Holt, A. F., & Becker, T. W. (2015). Anomalously fast convergence of India
942 and Eurasia caused by double subduction, 8(May). <https://doi.org/10.1038/NGEO2418>

943 Kapp, P., & Decelles, P. G. (2019). Mesozoic–Cenozoic geological evolution of the Himalayan-
944 Tibetan orogen and working tectonic hypotheses. *American Journal of Science*, 319(3), 159–
945 254. <https://doi.org/10.2475/03.2019.01>

946 Kapp, P., Yin, A., Harrison, T. M., & Ding, L. (2005). Cretaceous-Tertiary shortening , basin
947 development , and volcanism in central Tibet. *Geological Society of America Bulletin*, 117(7),
948 865–878. <https://doi.org/10.1130/B25595.1>

949 Khan, I. H., & Clyde, W. C. (2013). Lower Paleogene Tectonostratigraphy of Balochistan: Evidence
950 for Time-Transgressive Late Paleocene-Early Eocene Uplift. *Geosciences*, 3(5), 466–501.
951 <https://doi.org/10.3390/geosciences3030466>

952 Kohn, M. J., Parkinson, C. D., Kohn, M. J., & Parkinson, C. D. (2002). Petrologic case for Eocene
953 slab breakoff during the Indo-Asian collision. *Geology*, 30(7), 591–594.
954 [https://doi.org/10.1130/0091-7613\(2002\)030<0591](https://doi.org/10.1130/0091-7613(2002)030<0591)

955 Kopp, C., Fruehn, J., Flueh, E. R., Reichert, C., Kukowski, N., Bialas, J., & Klaeschen, D. (2000).
956 Structure of the makran subduction zone from wide-angle and reflection seismic data.
957 *Tectonophysics*, 329(1–4), 171–191. [https://doi.org/10.1016/S0040-1951\(00\)00195-5](https://doi.org/10.1016/S0040-1951(00)00195-5)

958 Kufner, S. K., Schurr, B., Haberland, C., Zhang, Y., Saul, J., Ischuk, A., & Oimahmadov, I. (2017).
959 Zooming into the Hindu Kush slab break-off: A rare glimpse on the terminal stage of
960 subduction. *Earth and Planetary Science Letters*, 461(October 2015), 127–140.
961 <https://doi.org/10.1016/j.epsl.2016.12.043>

962 Kufner, S. K., Kakar, N., Bezada, M., Bloch, W., Metzger, S., Yuan, X., et al. (2021). The Hindu
963 Kush slab break-off as revealed by deep structure and crustal deformation. *Nature*
964 *Communications*, 12(1), 1–11. <https://doi.org/10.1038/s41467-021-21760-w>

- 965 van de Lagemaat, S. H. A., van Hinsbergen, D. J. J., Boschman, L. M., Kamp, P. J. J., & Spakman,
966 W. (2018). Southwest Pacific Absolute Plate Kinematic Reconstruction Reveals Major Cenozoic
967 Tonga-Kermadec Slab Dragging. *Tectonics*, 37(8), 2647–2674.
968 <https://doi.org/10.1029/2017TC004901>
- 969 Lallemand, S., Heuret, A., Faccenna, C., & Funiciello, F. (2008). Subduction dynamics as revealed by
970 trench migration. *Tectonics*, 27(September 2007), 1–15. <https://doi.org/10.1029/2007TC002212>
- 971 Lee, C., & King, S. D. (2011). Dynamic buckling of subducting slabs reconciles geological and
972 geophysical observations. *Earth and Planetary Science Letters*, 312(3–4), 360–370.
973 <https://doi.org/10.1016/j.epsl.2011.10.033>
- 974 Lee, H., Chung, S., Lo, C., Ji, J., Lee, T., Qian, Q., & Zhang, Q. (2009). Tectonophysics Eocene
975 Neotethyan slab breakoff in southern Tibet inferred from the Linzizong volcanic record.
976 *Tectonophysics*, 477(1–2), 20–35. <https://doi.org/10.1016/j.tecto.2009.02.031>
- 977 Li, C., & Hilst, R. D. Van Der. (2010). Structure of the upper mantle and transition zone beneath
978 Southeast Asia from traveltimes tomography, 115, 1–19. <https://doi.org/10.1029/2009JB006882>
- 979 Li, C., Hilst, R. D. Van Der, Meltzer, A. S., & Engdahl, E. R. (2008). Subduction of the Indian
980 lithosphere beneath the Tibetan Plateau and Burma. *Earth and Planetary Science Letters*, 274,
981 157–168. <https://doi.org/10.1016/j.epsl.2008.07.016>
- 982 Li, S., Yin, C., Guilmette, C., Ding, L., & Zhang, J. (2019). Birth and demise of the Bangong-Nujiang
983 Tethyan Ocean : A review from the Gerze area of central Tibet. *Earth-Science Reviews*,
984 198(April), 102907. <https://doi.org/10.1016/j.earscirev.2019.102907>
- 985 Li, Zhen, Qiu, J., & Yang, X. (2014). Earth-Science Reviews A review of the geochronology and
986 geochemistry of Late Yanshanian (Cretaceous) plutons along the Fujian coastal area of
987 southeastern China : Implications for magma evolution related to slab break-off and rollback in
988 the Cretaceous. *Earth Science Reviews*, 128, 232–248.
989 <https://doi.org/10.1016/j.earscirev.2013.09.007>
- 990 Li, Zhenyu, Ding, L., Lippert, P. C., Song, P., Yue, Y., & Hinsbergen, D. J. J. Van. (2016).
991 Paleomagnetic constraints on the Mesozoic drift of the Lhasa terrane (Tibet) from Gondwana
992 to Eurasia. *Geology*, 44(9), 727–730. <https://doi.org/10.1130/G38030.1>
- 993 Lippert, P. C., Van Hinsbergen, D. J. J., & Dupont-Nivet, G. (2014). Early Cretaceous to present
994 latitude of the central proto-Tibetan Plateau: A paleomagnetic synthesis with implications for
995 Cenozoic tectonics, paleogeography, and climate of Asia. *Special Paper of the Geological*
996 *Society of America*, 507, 1–21. [https://doi.org/10.1130/2014.2507\(01\)](https://doi.org/10.1130/2014.2507(01))

- 997 Lister, G., Kennett, B., Richards, S., & Forster, M. (2008). Boudinage of a stretching slablet
998 implicated in earthquakes beneath the Hindu Kush. *Nature Geoscience*, 1(3), 196–201.
999 <https://doi.org/10.1038/ngeo132>
- 1000 Lithgow-bertelloni, C., & Richards, M. A. (1998a). The Dynamics Of Cenozoic And Mesozoic
1001 Motions. *Reviews of Geophysics*, 36(97), 27–78.
- 1002 Lithgow-bertelloni, C., & Richards, M. A. (1998b). The Dynamics Of Cenozoic And Mesozoic
1003 Motions. *Reviews of Geophysics*, (97), 27–78.
- 1004 Luo, A. B., & Fan, J. J. (2020). Aptian Flysch in Central Tibet : Constraints on the Timing of Closure
1005 of the Bangong - Nujiang Tethyan Ocean. *Tectonics*, 39. <https://doi.org/10.1029/2020TC006198>
- 1006 Magni, V., Allen, M. B., Hunen, J. Van, & Bouilhol, P. (2017). Continental underplating after slab
1007 break-off. *Earth and Planetary Science Letters*, 474, 59–67.
1008 <https://doi.org/10.1016/j.epsl.2017.06.017>
- 1009 Maheo, G., Guillot, S., Blichert-toft, J., Rolland, Y., & Pe, A. (2002). A slab breakoff model for the
1010 Neogene thermal evolution of South Karakorum and South Tibet. *Earth and Planetary Science
1011 Letters*, 195.
- 1012 Martin, C. R., Jagoutz, O., Upadhyay, R., Royden, L. H., Eddy, M. P., Bailey, E., et al. (2020).
1013 Paleocene latitude of the Kohistan – Ladakh arc indicates multistage India – Eurasia collision.
1014 *PNAS*, 117(47). <https://doi.org/10.1073/pnas.2009039117>
- 1015 Maury, C., Coulon, C., Megartsi, M., Fourcade, S., Louni-hacini, A., Cotten, J., et al. (2002). Post-
1016 collisional transition from calc-alkaline to alkaline volcanism during the Neogene in Oranie (
1017 Algeria): magmatic expression of a slab breakoff. *LITHOS*, 62, 87–110.
- 1018 van der Meer, D. G., van Hinsbergen, D. J. J., & Spakman, W. (2018). Atlas of the underworld: Slab
1019 remnants in the mantle, their sinking history, and a new outlook on lower mantle viscosity.
1020 *Tectonophysics*, 723(June 2017), 309–448. <https://doi.org/10.1016/j.tecto.2017.10.004>
- 1021 Van Der Meer, D. G., Spakman, W., Van Hinsbergen, D. J. J., Amaru, M. L., & Torsvik, T. H.
1022 (2010). Towards absolute plate motions constrained by lower-mantle slab remnants. *Nature
1023 Geoscience*, 3(1), 36–40. <https://doi.org/10.1038/ngeo708>
- 1024 Van Der Meer, D. G., Zeebe, R. E., Hinsbergen, D. J. J. Van, Sluijs, A., & Spakman, W. (2014). Plate
1025 tectonic controls on atmospheric CO₂ levels since the Triassic. *PNAS*, 111(12).
1026 <https://doi.org/10.1073/pnas.1315657111>
- 1027 Meulen, M. J. Van Der, Meulenkamp, J. E., & Wortel, M. J. R. (1998). Lateral shifts of Apenninic
1028 foredeep depocentres reflecting detachment of subducted lithosphere. *Earth and Planetary*

- 1029 *Science Letters*, 154, 203–219.
- 1030 Miller, M. S., Gorbatov, A., & Kennett, B. L. N. (2005). Heterogeneity within the subducting Pacific
1031 slab beneath the Izu-Bonin-Mariana arc: Evidence from tomography using 3D ray tracing
1032 inversion techniques. *Earth and Planetary Science Letters*, 235(1–2), 331–342.
1033 <https://doi.org/10.1016/j.epsl.2005.04.007>
- 1034 Molnar, P., & Stock, J. M. (2009). Slowing of India's convergence with Eurasia since 20 Ma and its
1035 implications for Tibetan mantle dynamics. *Tectonics*, 28(3), 1–11.
1036 <https://doi.org/10.1029/2008TC002271>
- 1037 Molnar, P., & tapponnier, P. (1975). Cenozoic Tectonics of Asia: Effects of a Continental Collision.
1038 *Science*, 189(4201), 419–426.
- 1039 Morley, C. K., & Arboit, F. (2019). Dating the onset of motion on the Sagaing fault : Evidence from
1040 detrital zircon and titanite U-Pb geochronology from the North Minwun Basin , Myanmar,
1041 47(6), 581–585.
- 1042 Murphy, M. A., Harrison, T. M., Wang, X., & Zhou, X. (1997). Did the Indo-Asian collision alone
1043 create the Tibetan plateau ? *Geology*, 25(8), 719–722.
- 1044 Nábelek, J., Hetényi, G., Vergne, J., Sapkot, S., Kafle, B., Jiang, M., et al. (2009). Underplating in the
1045 Himalaya-Tibet Collision Zone Revealed by the Hi-CLIMB Experiment Underplating in the
1046 Himalaya-Tibet Collision Zone Revealed by the Hi-CLIMB Experiment. *Science*, 325(October).
1047 <https://doi.org/10.1126/science.1167719>
- 1048 Najman, Y., Appel, E., Fadel, M. B., Bown, P., Carter, A., Garzanti, E., et al. (2010). Timing of India
1049 - Asia collision : Geological , biostratigraphic , and palaeomagnetic constraints. *Journal of*
1050 *Geophysical Research*, 115(B12416), 1–18. <https://doi.org/10.1029/2010JB007673>
- 1051 Negredo, A. M., Replumaz, A., Villaseñor, A., & Guillot, S. (2007). Modeling the evolution of
1052 continental subduction processes in the Pamir – Hindu Kush region. *Earth and Planetary*
1053 *Science Letters*, 259, 212–225. <https://doi.org/10.1016/j.epsl.2007.04.043>
- 1054 Ninkabou, D., Agard, P., Nielsen, C., Smit, J., & Gorini, C. (2021). Structure of the offshore obducted
1055 Oman margin: emplacement of Semail ophiolite and role of tectonic inheritance. *Journal of*
1056 *Geophysical Research Solid Earth*, 126(2). <https://doi.org/10.1029/2020JB020187>
- 1057 Parsons, A. J., Hosseini, K., Palin, R., & Sigloch, K. (2020). Geological, geophysical and plate
1058 kinematic constraints for models of the India-Asia collision and the post-Triassic central Tethys
1059 oceans. *Earth-Science Reviews*, 202(January), 103084.
1060 <https://doi.org/10.1016/j.earscirev.2020.103084>

- Parsons, A. J., Sigloch, K., & Hosseini, K. (2021). Australian plate subduction is responsible for northward motion of the India- Asia collision zone and ~ 1000 km lateral migration of the Indian slab. *Geophysical Research Letters*, 48(18).
- Patriat, P., & Achache, J. (1984). India-Eurasia collision chronology has implications for crustal shortening and driving mechanism of plates. *Nature*.
- Plunder, A., Bandyopadhyay, D., Ganerød, M., & Advokaat, E. L. (2020). History of Subduction Polarity Reversal During Arc - Continent Collision : Constraints From the Andaman Ophiolite and its Metamorphic Sole. *Tectonics*, 39, 1–24. <https://doi.org/10.1029/2019TC005762>
- Regard, V., Faccenna, C., Bellier, O., & Martinod, J. (2008). Laboratory experiments of slab break-off and slab dip reversal : insight into the Alpine Oligocene reorganization. *Terra Nova*, 20, 267–273. <https://doi.org/10.1111/j.1365-3121.2008.00815.x>
- Replumaz, Negredo, A. M., Guillot, S., & Villaseñor, A. (2010). Multiple episodes of continental subduction during India/Asia convergence: Insight from seismic tomography and tectonic reconstruction. *Tectonophysics*, 483(1–2), 125–134. <https://doi.org/10.1016/j.tecto.2009.10.007>
- Replumaz, A., & Tapponnier, P. (2003). Reconstruction of the deformed collision zone Between India and Asia by backward motion of lithospheric blocks. *Journal of Geophysical Research: Solid Earth*, 108(B6). <https://doi.org/10.1029/2001jb000661>
- Replumaz, Anne, Kárasón, H., van der Hilst, R. D., Besse, J., & Tapponnier, P. (2004). 4-D evolution of SE Asia's mantle from geological reconstructions and seismic tomography. *Earth and Planetary Science Letters*, 221(1–4), 103–115. [https://doi.org/10.1016/S0012-821X\(04\)00070-6](https://doi.org/10.1016/S0012-821X(04)00070-6)
- Replumaz, Anne, Guillot, S., Villaseñor, A., & Negredo, A. M. (2013). Amount of Asian lithospheric mantle subducted during the India / Asia collision. *Gondwana Research*, 24(3–4), 936–945. <https://doi.org/10.1016/j.gr.2012.07.019>
- Replumaz, Anne, Capitanio, F. A., Guillot, S., Negredo, A. M., & Villaseñor, A. (2014). The coupling of Indian subduction and Asian continental tectonics. *Gondwana Research*, 26(2), 608–626. <https://doi.org/10.1016/j.gr.2014.04.003>
- Richards, M. A., & Engebretson, D. C. (1990). Large-scale mantle convection and the history of subduction, 4, 437–440.
- Rodriguez, M., Chamot-rooke, N., Huchon, P., & Fournier, M. (2014). Tectonics of the Dalrymple Trough and uplift of the Murray Ridge (NW Indian Ocean). *Tectonophysics*, (October 2017). <https://doi.org/10.1016/j.tecto.2014.08.001>
- Royden, L. H. (1993). Evolution Of Retreating Subduction Boundaries Formed During Continental

- 1093 Collision, *12*(3), 629–638.
- 1094 Royden, L. H., Burchfiel, B. C., & Hilst, R. D. Van Der. (2008). of the Tibetan Plateau. *Science*,
1095 *321*(August), 1054–1058.
- 1096 Schellart, W. P. (2008). Subduction zone trench migration: Slab driven or overriding-plate-driven?
1097 *Physics of the Earth and Planetary Interiors*, *170*(1–2), 73–88.
1098 <https://doi.org/10.1016/j.pepi.2008.07.040>
- 1099 Schellart, W. P., & Spakman, W. (2015). Australian plate motion and topography linked to fossil New
1100 Guinea slab below Lake Eyre. *Earth and Planetary Science Letters*, *421*, 107–116.
1101 <https://doi.org/10.1016/j.epsl.2015.03.036>
- 1102 Schepers, G., Van Hinsbergen, D. J. J., Spakman, W., Kesters, M. E., Boschman, L. M., &
1103 McQuarrie, N. (2017). South-American plate advance and forced Andean trench retreat as
1104 drivers for transient flat subduction episodes. *Nature Communications*, *8*(0316), 1–9.
1105 <https://doi.org/10.1038/ncomms15249>
- 1106 Sdrolias, M., & Müller, R. D. (2006). Controls on back-arc basin formation. *Geochemistry*,
1107 *Geophysics, Geosystems*, *7*(4). <https://doi.org/10.1029/2005GC001090>
- 1108 Shephard, G. E., Matthews, K. J., Hosseini, K., & Domeier, M. (2017). On the consistency of
1109 seismically imaged lower mantle slabs. *Scientific Reports*, *7*(1), 1–17.
1110 <https://doi.org/10.1038/s41598-017-11039-w>
- 1111 Sigloch, K., & Mihalynuk, M. G. (2013). Intra-oceanic subduction shaped the assembly of Cordilleran
1112 North America. *Nature*, *496*(7443), 50–56. <https://doi.org/10.1038/nature12019>
- 1113 Song, P., Ding, L., Li, Z., Lippert, P. C., & Yue, Y. (2017). An early bird from Gondwana:
1114 Paleomagnetism of Lower Permian lavas from northern Qiangtang (Tibet) and the geography of
1115 the Paleo-Tethys. *Earth and Planetary Science Letters*, *475*(October), 119–133.
1116 <https://doi.org/10.1016/j.epsl.2017.07.023>
- 1117 spakman, W., Wortel, M. J. R., & Vlaar, N. J. (1988). The Hellenic Subduction Zone: A Tomographic
1118 Image And Its Geodynamic Implications. *Geophysical Research Letters*, *15*(1), 60–63.
- 1119 Spakman, W., Chertova, M. V, Van Den Berg, A., & Van Hinsbergen, D. J. J. (2018). Puzzling
1120 features of western Mediterranean tectonics explained by slab dragging. *Nature Geoscience*,
1121 *11*(3), 211–216. <https://doi.org/10.1038/s41561-018-0066-z>
- 1122 Sperner, B., Lorenz, F., Bonjer, K., Hettel, S., Müller, B., & Wenzel, F. (2001). Slab break-off -
1123 Abrupt cut or gradual detachment? New insights from the Vrancea Region (SE Carpathians,
1124 Romania). *Terra Nova*, *13*(3), 172–179. <https://doi.org/10.1046/j.1365-3121.2001.00335.x>

- 1125 Torsvik, T. H., Van der Voo, R., Preeden, U., Mac Niocaill, C., Steinberger, B., Doubrovine, P. V., et
1126 al. (2012). Phanerozoic Polar Wander, Palaeogeography and Dynamics. *Earth-Science Reviews*,
1127 *114*(3–4), 325–368. <https://doi.org/10.1016/j.earscirev.2012.06.007>
- 1128 Torsvik, T. H., Voo, R. Van Der, Doubrovine, P. V, Burke, K., & Steinberger, B. (2014). Deep
1129 mantle structure as a reference frame for movements in and on the Earth. *PNAS*, *111*(24).
1130 <https://doi.org/10.1073/pnas.1318135111>
- 1131 Torsvik, T. H., Steinberger, B., & Shephard, G. E. (2019). Pacific - Panthalassic Reconstructions :
1132 Overview , Errata and the Way Forward Geochemistry , Geophysics , Geosystems.
1133 *Geochemistry Geophysics Geosystems*, *20*, 3659–3689. <https://doi.org/10.1029/2019GC008402>
- 1134 Vissers, R. L. M., van Hinsbergen, D. J. J., van der Meer, D. G., & Spakman, W. (2016). Cretaceous
1135 slab break-off in the Pyrenees: Iberian plate kinematics in paleomagnetic and mantle reference
1136 frames. *Gondwana Research*, *34*, 49–59. <https://doi.org/10.1016/j.gr.2016.03.006>
- 1137 Van Der Voo, R., Spakman, W., & Bijwaard, H. (1999). Tethyan subducted slabs under India. *Earth
1138 and Planetary Science Letters*, *171*(1), 7–20. [https://doi.org/10.1016/S0012-821X\(99\)00131-4](https://doi.org/10.1016/S0012-821X(99)00131-4)
- 1139 Van Der Voo, R., Van Hinsbergen, D. J. J., Domeier, M., Spakman, W., & Torsvik, T. H. (2015).
1140 Latest Jurassic-earliest Cretaceous closure of the Mongol-Okhotsk Ocean: A paleomagnetic and
1141 seismological-tomographic analysis. *Special Paper of the Geological Society of America*,
1142 *513*(June), 589–606. [https://doi.org/10.1130/2015.2513\(19\)](https://doi.org/10.1130/2015.2513(19))
- 1143 Westerweel, J., Roperch, P., Licht, A., Dupont-Nivet, G., Win, Z., Poblete, F., et al. (2019). Burma
1144 Terrane part of the Trans-Tethyan arc during collision with India according to palaeomagnetic
1145 data. *Nature Geoscience*, *12*(10), 863–868. <https://doi.org/10.1038/s41561-019-0443-2>
- 1146 Wortel, M. J. R., & Spakman, W. (1992). Structure and dynamic of subducted lithosphere in the
1147 Mediterranean. *Proc. Kon. Ned. Akad. v. Wetensch*, *95*(3), 325–347.
- 1148 Wortel, M. J. R., & Spakman, W. (2000). Subduction and slab detachment in the Mediterranean-
1149 Carpathian region. *Science*, *290*(5498), 1910–1917.
1150 <https://doi.org/10.1126/science.290.5498.1910>
- 1151 Wu, J., Suppe, J., Lu, R., & Kanda, R. (2016). Philippine Sea and East Asian plate tectonics since 52
1152 Ma constrained by new subducted slab reconstruction methods. *Journal of Geophysical
1153 Research: Solid Earth*, *121*(6), 4670–4741. <https://doi.org/10.1002/2016JB012923>
- 1154 Yamini-Fard, F., Hatzfeld, D., Farahbod, A. M., Paul, A., & Mokhtari, M. (2007). The diffuse
1155 transition between the Zagros continental collision and the Makran oceanic subduction (Iran):
1156 microearthquake seismicity and crustal structure. *Geophysical Journal International*, *170*, 182–

1157 194. <https://doi.org/10.1111/j.1365-246X.2006.03232.x>

1158 Yin, A., & Harrison, T. M. (2000). Geologic Evolution Of The Himalayan - Tibetan Oogen. *Annu.*
1159 *Rev. Earth Planet. Sci*, 28, 211–80.

1160 Yoshioka, S., & Wortel, M. J. R. (1995). Three-dimensional numerical modeling of detachment of
1161 subducted lithosphere. *Journal of Geophysical Research*, 100(B10).
1162 <https://doi.org/10.1029/94jb01258>

1163 Yuan, C., Sun, M., Wilde, S., Xiao, W., Xu, Y., Long, X., & Zhao, G. (2010). Lithos Post-collisional
1164 plutons in the Balikun area , East Chinese Tianshan : Evolving magmatism in response to
1165 extension and slab break-off. *LITHOS*, 119(3–4), 269–288.
1166 <https://doi.org/10.1016/j.lithos.2010.07.004>

1167 van de Zedde, D. M. A., & Wortel, M. J. R. (2001). Shallow slab detachment as a transient source of
1168 heat at midlithospheric depths. *Tectonics*, 20(6), 868–882.
1169 <https://doi.org/10.1029/2001TC900018>

1170 Zhao, D., & Ohtani, E. (2009). Deep slab subduction and dehydration and their geodynamic
1171 consequences : Evidence from seismology and mineral physics. *Gondwana Research*, 16(3–4),
1172 401–413. <https://doi.org/10.1016/j.gr.2009.01.005>

1173 Zhu, D., Wang, Q., Zhao, Z., Chung, S., Cawood, P. A., Niu, Y., et al. (2015). Magmatic record of
1174 India-Asia collision. *Nature Scientific Reports*, 1–9. <https://doi.org/10.1038/srep14289>

1175 Zhu, D., Li, S., Cawood, P. A., Wang, Q., Zhao, Z., Liu, S., & Wang, L. (2016). Assembly of the
1176 Lhasa and Qiangtang terranes in central Tibet by divergent double subduction. *LITHOS*, 245, 7–
1177 17. <https://doi.org/10.1016/j.lithos.2015.06.023>

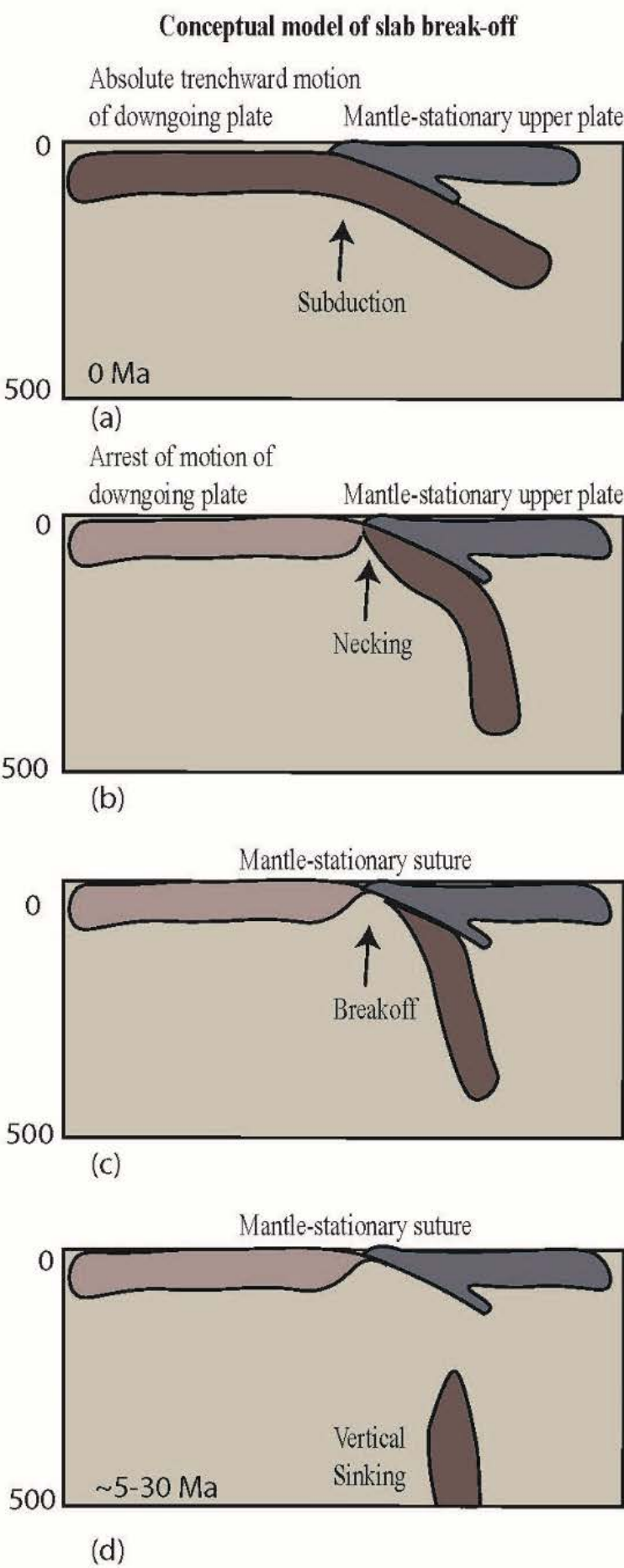


Figure 1: Comparison of the shallow slab break off conceptual numerical model (a-d) (Duretz et al., 2011) vs proposed slab shear off model of Indian & Eurasian plate. It is observed that slab break off numerical models are different to reality (Static Trench vs Trench Advance). (a) represents the oceanic subduction, (b) represents continental collision, (c) represents necking and break off respectively (d) represents the post break off rebound.

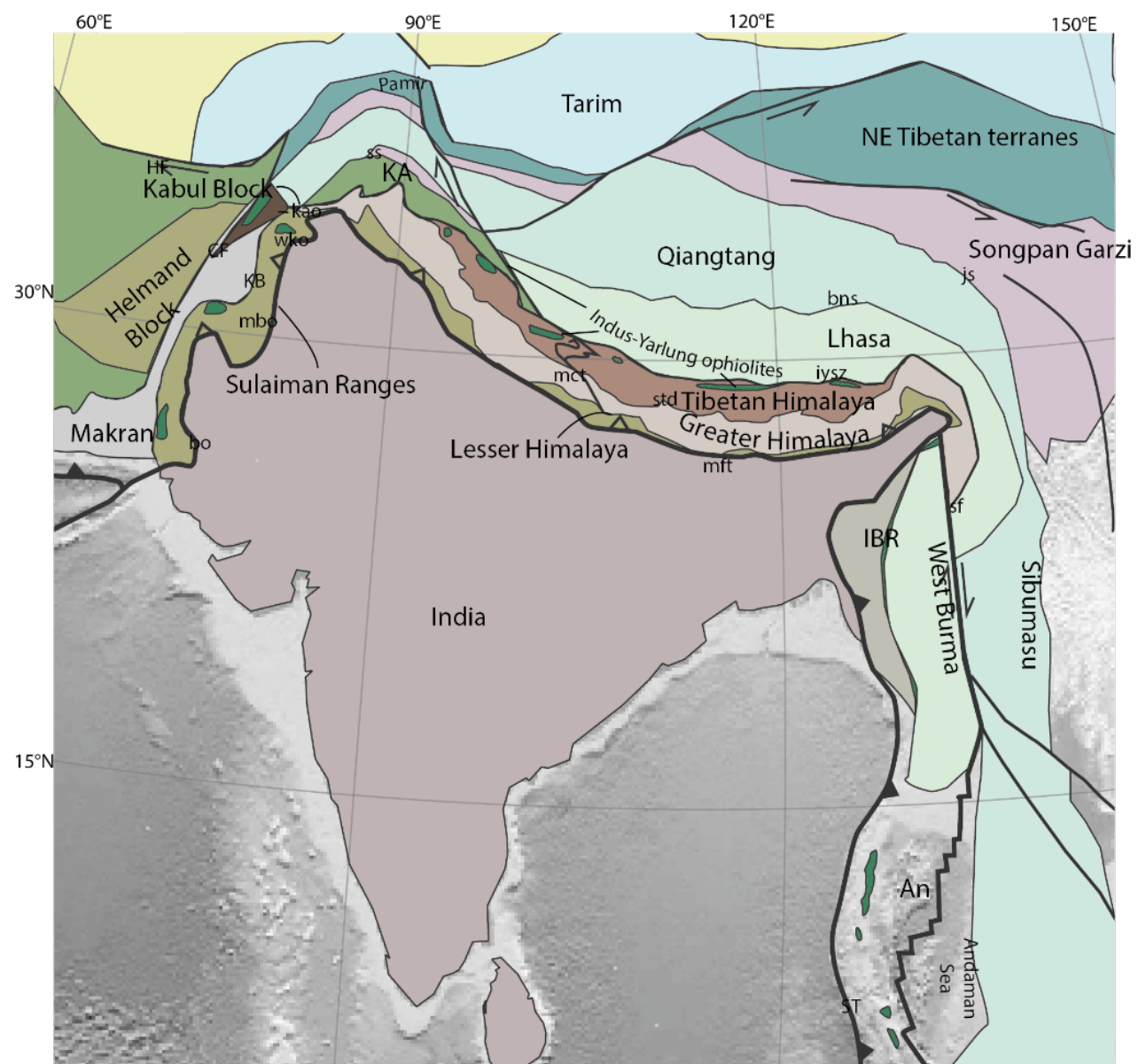
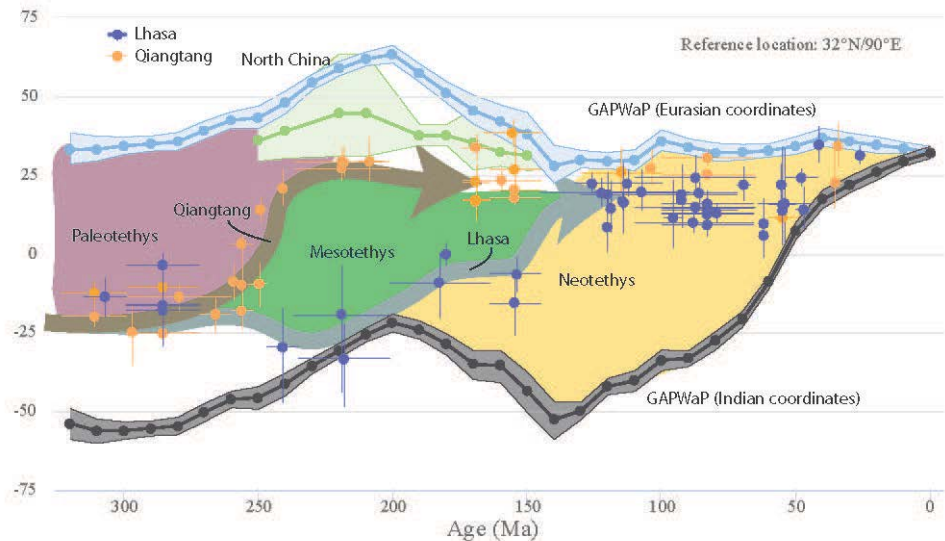


Figure 2. Tectonic Map of the Asian-India collision region. Abbreviations are: An=Andaman Islands;; bns=Bangong-Nujiang Suture; bo=Bela Ophiolite; CF=Chaman Fault; HF=Herat Fault; MFT=Main

1200 Frontal Thrust; IBR=Indo-Burman Ranges; IYSZ=Indus-Yarlung Suture Zone; KA=Kohistan Arc;
1201 kao=Kabul-Altimur Ophiolite; KB=Ka- tawaz Basin; js=Jinsha Suture; mbo=Muslim Bagh Ophiolite;
1202 mct=Main Central Thrust; mft=Main Frontal Thust; SF=Sagaing Fault; SS=Shyok Suture; ST=Sunda
1203 Trench; std.=South Tibetan Detachment; wko=Waziristan-Khost Ophiolite.

1204



1205

1206 Figure 3. Paleolatitude curves for a reference point (32°N, 90°E). Each curve shows a paleolatitude
1207 predicted for the reference point by the Global Apparent Polar Wander Path of Torsvik et al. (2012),
1208 assuming the reference point was rigidly connected to Eurasia (blue curve), Lhasa (orange curve), and
1209 India (black curve). Each curve indicate a lost ocean and relevent lithosphere in between and marked
1210 with different colors.

1211

Slab shape as function of absolute slab and trench motion during subduction

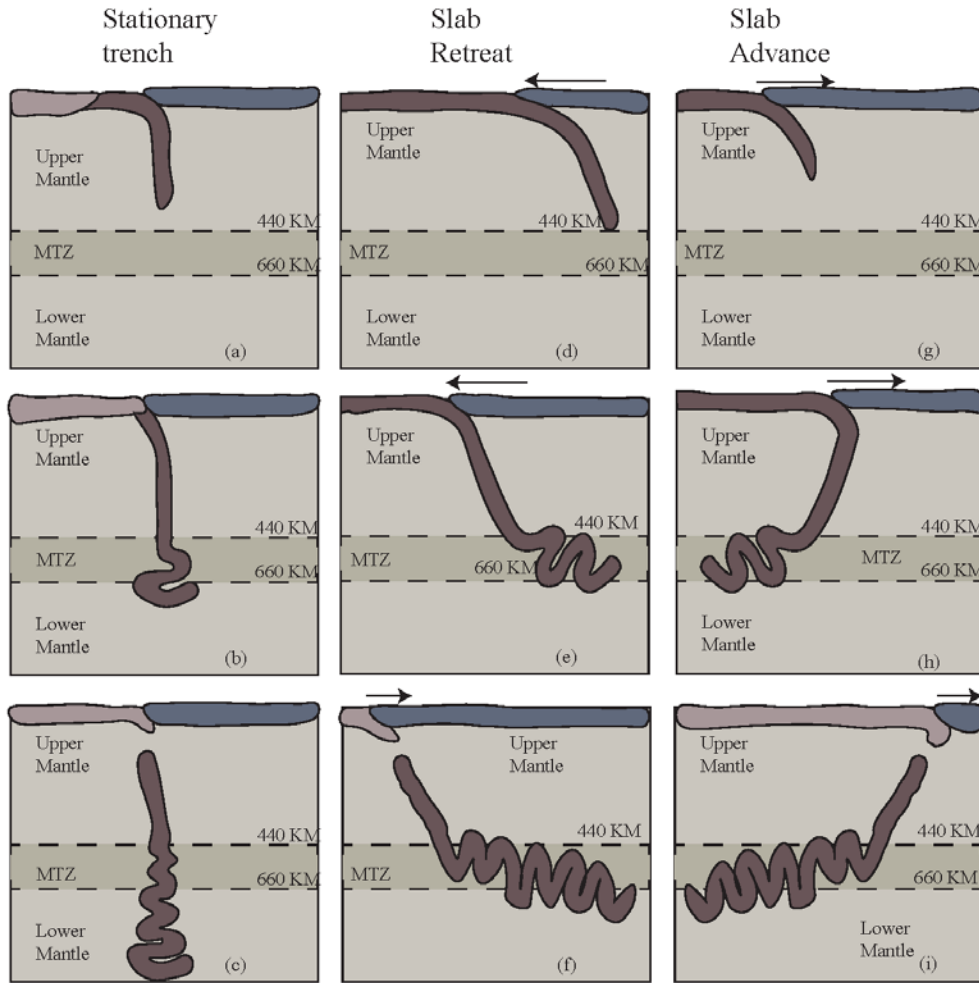


Figure 4: Conceptual models of the Slab detachment (g-i) as compared with existing models of slab breakoff in various subduction scenarios(a-c, d-f) (Parsons et al., 2020). Proposed Trench Advance model indicating trench moving forward and leaving detached slab behind in the mantle (g-l) oceanic crust, continental crust and overriding plates are coloured in separate colours.

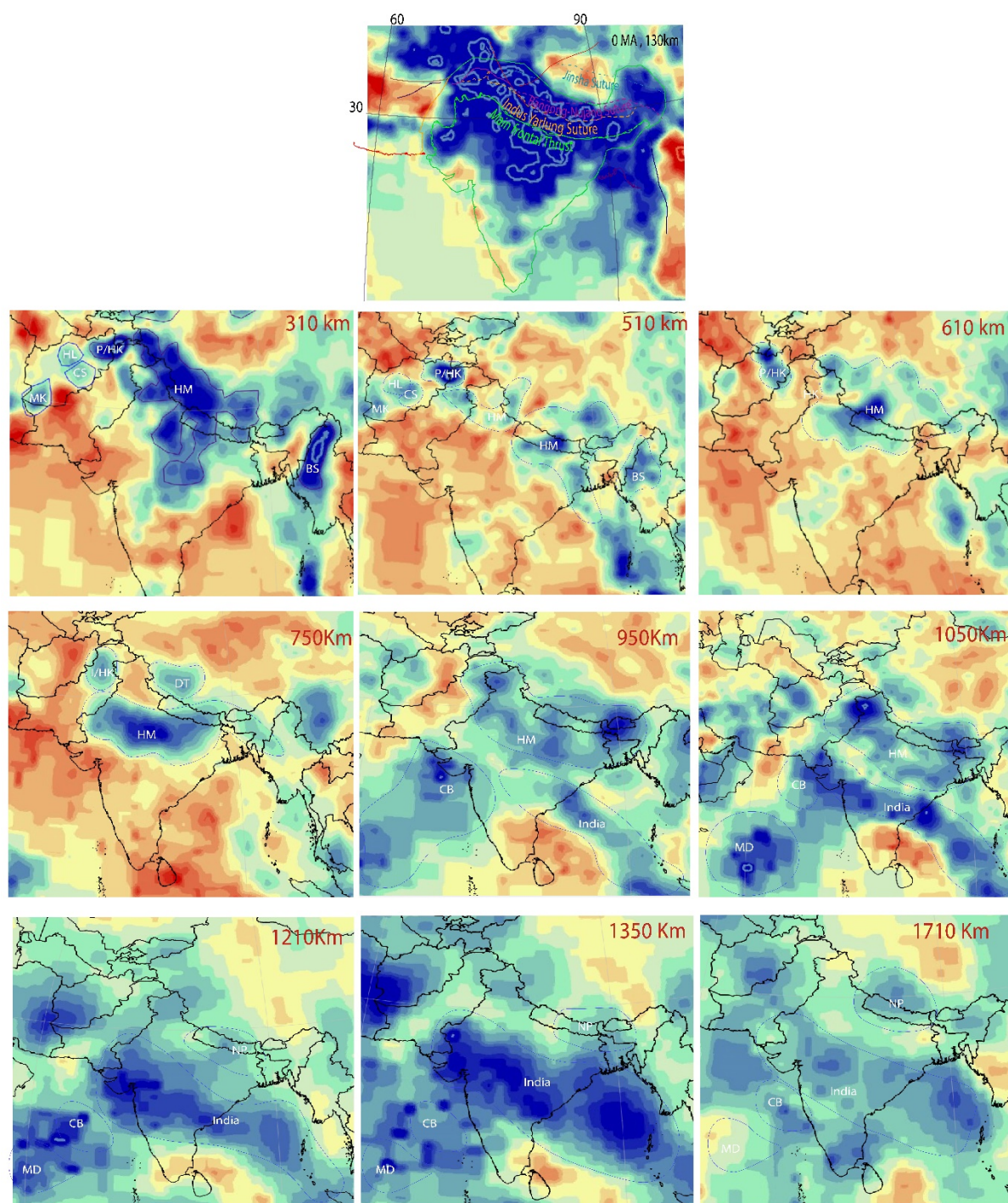


Figure 5: Tomographic Horizontal sections indicating the relative positions and geometric variations of anomalies. Hm: Himalaya Anomaly, India: India Anomaly, MD: Maldives anomaly, BS: Burma Slab, CC: Central China anomaly, CS: Chaman Slab NP=Nepal anomaly, DT= Detached Tibet, Tarim & Kazak= Tarim & Kazak Anomaly, Arabia/CB= Carlsberg anomaly, HI= Helmand anomaly, MK= Makran anomaly . Line of section in shown in the inset map.

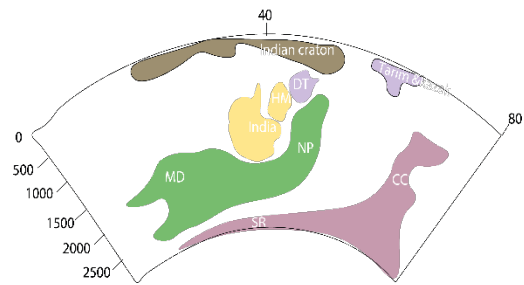
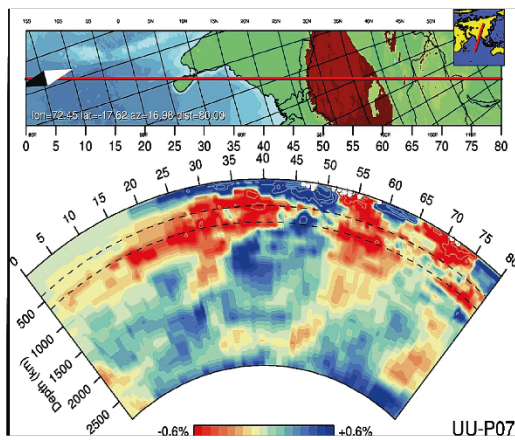
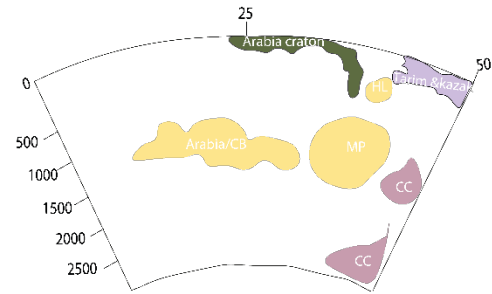
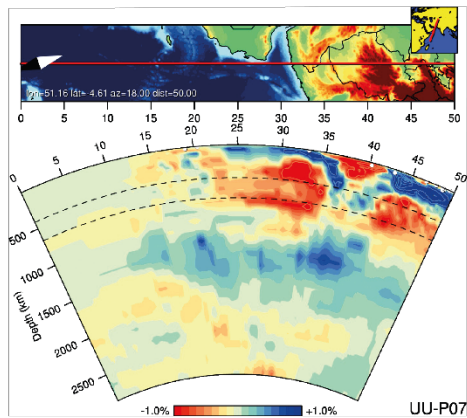


Figure 6: Cross section through the tomography model UU-P07. Labels display the positions of anomalies. Hm: Himalaya Anomaly, India: India Anomaly, MD: Maldives anomaly, BS: Burma Slab, CC Central China anomaly, NP=Nepal anomaly, DT= Detached Tibet, Tarim & Kazak= Tarim & Kazak Anomaly, Arabia/CB= Carlsberg anomaly, HL= Helmand anomaly, MK= Makran anomaly, SR= Sri Lanka Anomaly . Line of section in shown in the inset map.

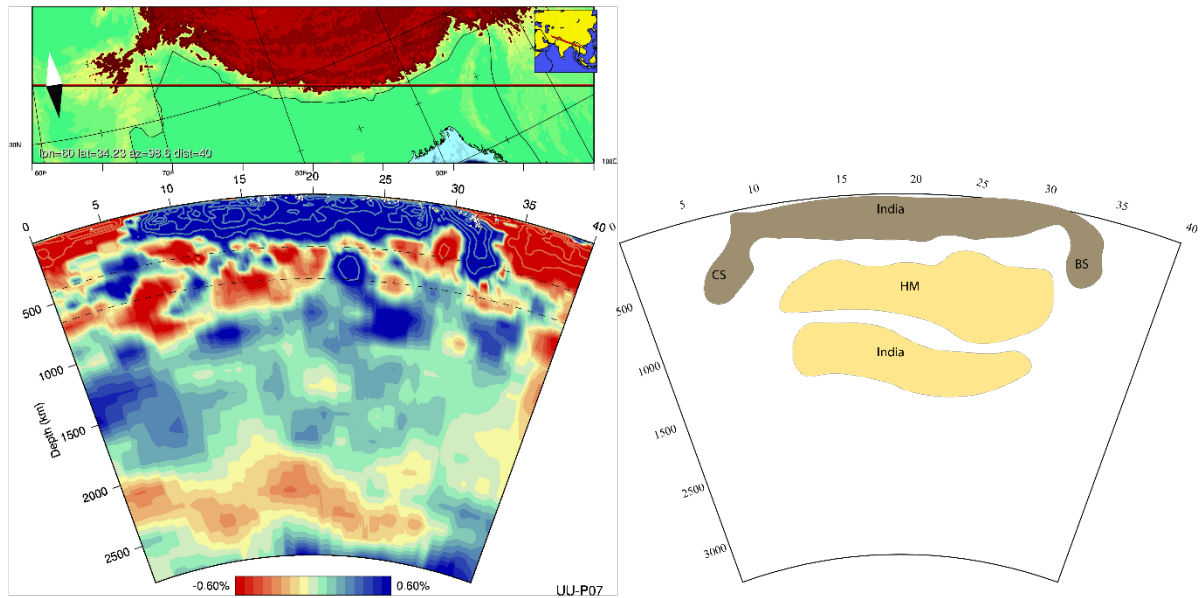


Figure 7: E-W Tomographic section through northern Indian plate. Oblique subduction is observed at the western and eastern margin of Indian plate. BS=Burma Slab, CS= Chaman slab, HM= Himalaya slab.

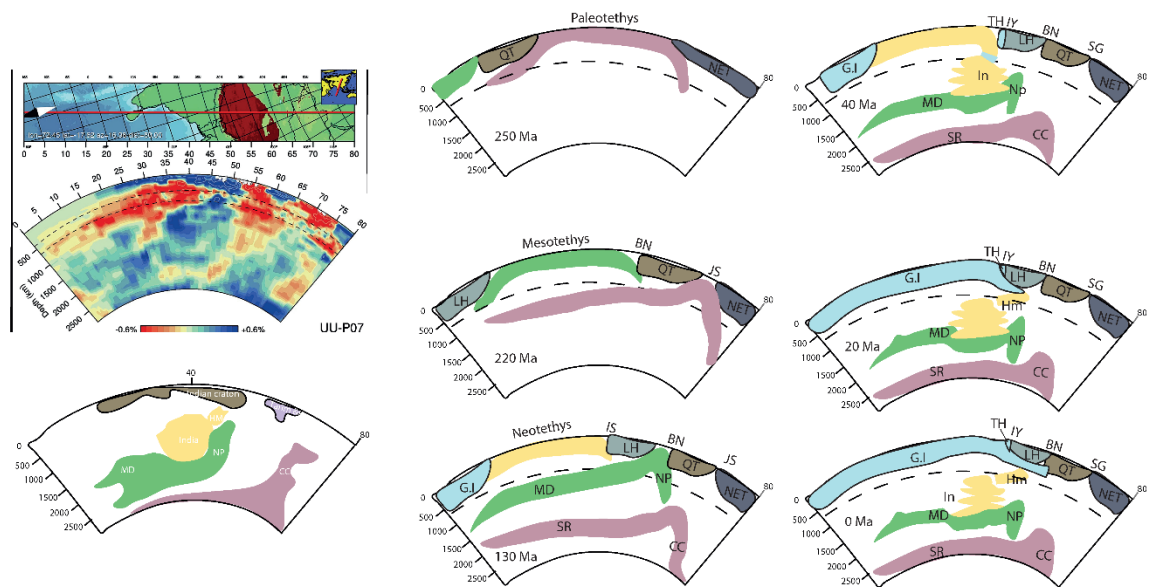


Figure 8: Interpreted models of the subducted slabs since 250 Ma and their comparison with the reference tomographic interpretation (on left). At the present day configuration PaleoTethys slabs (pink)

can be found deep in the mantle at the Core mantle boundary, MesoTethys slabs (green) are just above followed by the Neo Tethys slabs (Yellow). Notice the trench advance during all the subduction scenarios.

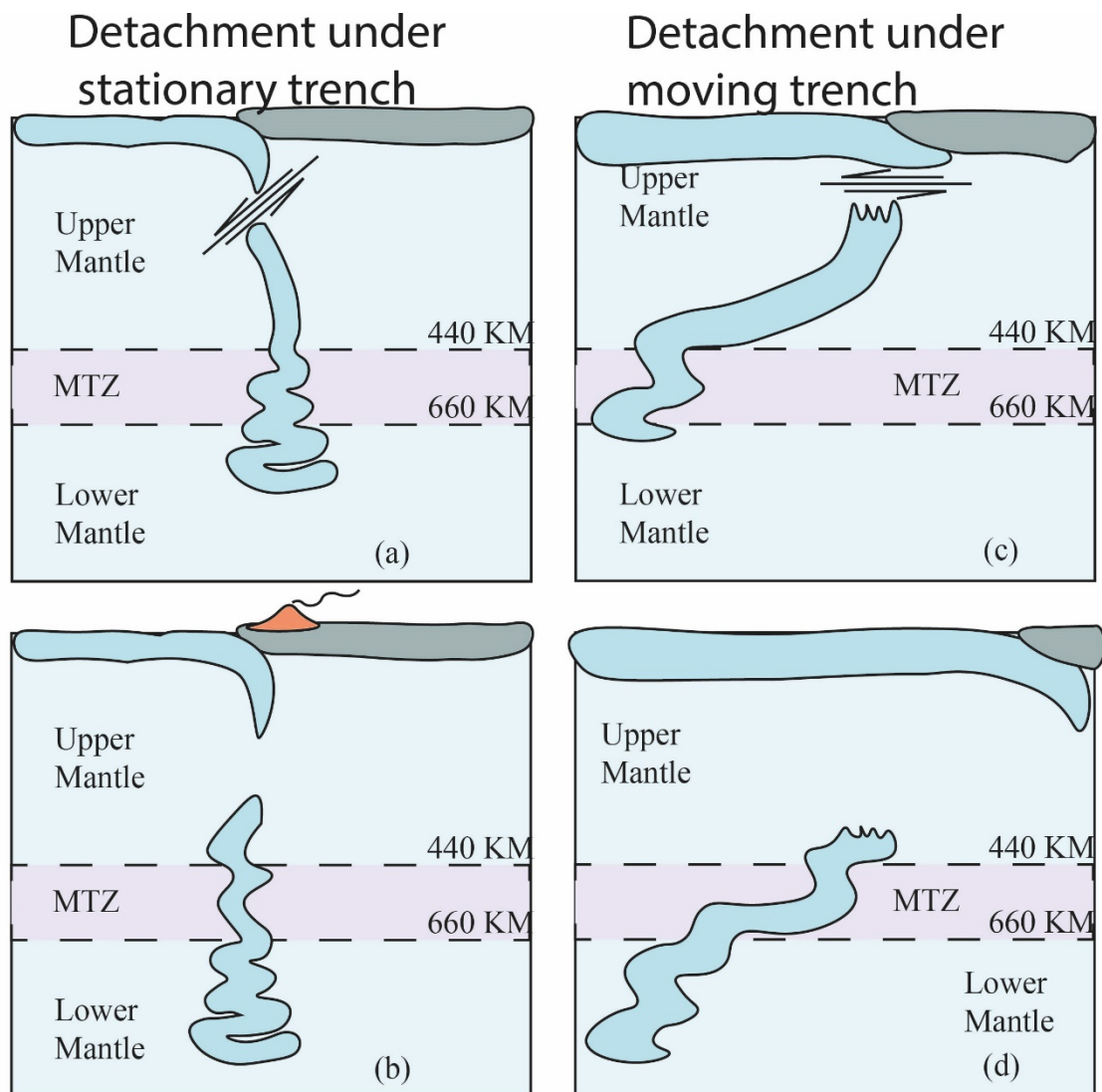


Figure 9: Comparison of Detachment under stationary trench against Detachment under moving trench. Notice the sub vertical shear in the Detachment under stationary and the sub horizontal shear in case of Detachment under moving trench. Detachment under stationary is followed by the volcanism and Detachment under moving trench is followed by the trench advance resulting in possibly overturned slab.

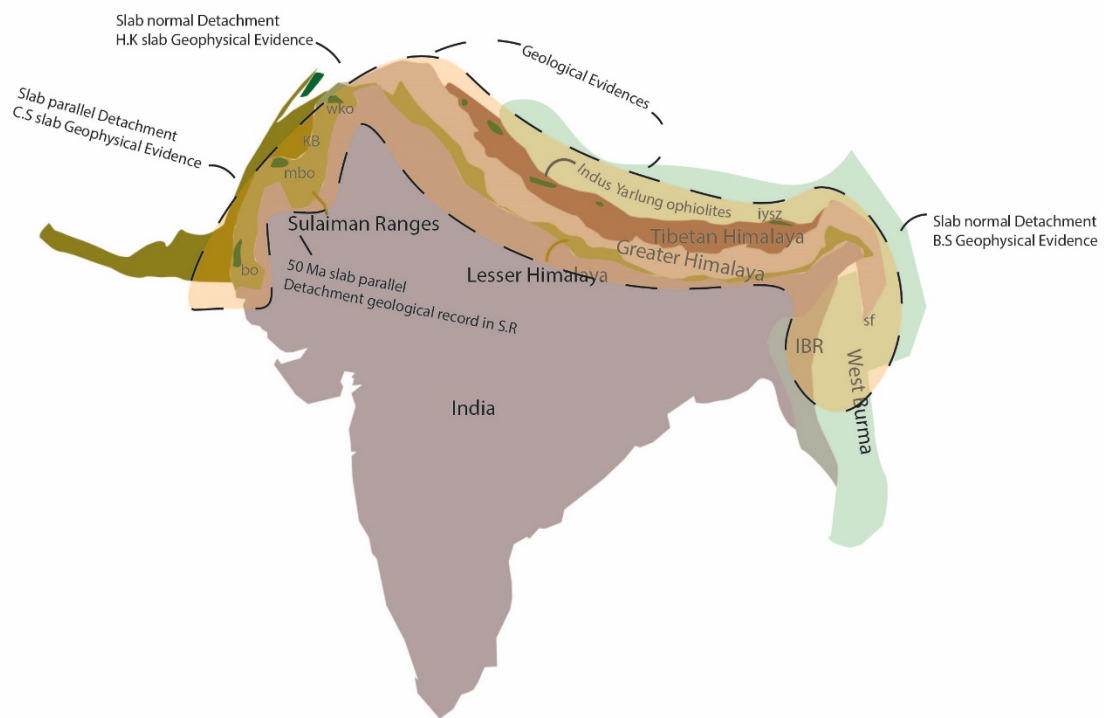


Figure 10: Map indicating the future Geological and Geophysical learning opportunities in the study area. Geological and Geophysical evidences can be compared to resolve the complex nature of subduction during India- Asia collision.